Atmospheric Research 203 (2018) 141–163

Contents lists available at ScienceDirect

Atmospheric Research

journal homepage: www.elsevier.com/locate/atmosres

Detection of spatio-temporal variability of air temperature and precipitation based on long-term meteorological station observations over Tianshan Mountains, Central Asia

Min Xu[a,b], Shichang Kang[a,c,*], Hao Wu[d], Xu Yuan[b]

[a] State Key Laboratory of Cryospheric Science, Northwest Institute of Eco-Environment and Resources, Chinese Academy of Sciences, Lanzhou 730000, China
[b] Faculty of Geo-Information Science and Earth Observation, University of Twente, Enschede 7513BH, Netherlands
[c] CAS Center for Excellence in Tibetan Plateau Earth Sciences, Chinese Academy of Sciences, Beijing 100101, China
[d] State Key Laboratory of Water Resources and Hydropower Engineering Science, Wuhan University, Wuhan 430072, China

ARTICLE INFO

Keywords:
Tianshan Mountains
Air temperature and precipitation
Mann-Kendall test
Mutations
Periodicity
Elevation dependency

ABSTRACT

As abundant distribution of glaciers and snow, the Tianshan Mountains are highly vulnerable to changes in climate. Based on meteorological station records during 1960–2016, we detected the variations of air temperature and precipitation by using non-parametric method in the different sub-regions and different elevations of the Tianshan Mountains. The mutations of climate were investigated by Mann-Kendall abrupt change test in the sub-regions. The periodicity is examined by wavelet analysis employing a chi-square test and detecting significant time sections. The results show that the Tianshan Mountains experienced an overall rapid warming and wetting during study period, with average warming rate of 0.32 °C/10a and wet rate of 5.82 mm/10a, respectively. The annual and seasonal spatial variation of temperature showed different scales in different regions. The annual precipitation showed non-significant upward trend in 20 stations, and 6 stations showed a significant upward trend. The temperatures in the East Tianshan increased most rapidly at rates of 0.41 °C/10a. The increasing magnitudes of annual precipitation were highest in the Boertala Vally (8.07 mm/10a) and lowest in the East Tianshan (2.64 mm/10a). The greatest and weakest warming was below 500 m (0.42 °C/10a) and elevation of 1000–1500 m (0.23 °C/10a), respectively. The increasing magnitudes of annual precipitation were highest in the elevation of 1500 m–2000 m (9.22 mm/10a) and lowest in the elevation of below 500 m (3.45 mm/10a). The mutations of annual air temperature and precipitation occurred in 1995 and 1990, respectively. The large atmospheric circulation influenced on the mutations of climate. The significant periods of air temperature were 2.4–4.1 years, and annual precipitation was 2.5–7.4 years. Elevation dependency of temperature trend magnitude was not evidently in the Tianshan Mountains. The annual precipitation wetting trend was amplified with elevation in summer and autumn. The strong elevation dependence of precipitation increasing trend appeared in summer.

1. Introduction

Global warming trend is obviously during the past century and has been the topic of climate change (Alexander et al., 2006; Hansen et al., 2006; Gay-Garcia et al., 2009; Wen et al., 2017). The Intergovernmental Panel on Climate Change (IPCC) indicated that the global warming has caused changes of precipitation, contrasted in precipitation between wet and dry regions and between wet and dry seasons increased (IPCC AR5, 2013). Global land precipitation increased by approximately 2% over the 20th century (New et al., 2001). Previous studies suggested that changes of air temperature and precipitation are considerably diverse patterns from the tempo-spatial trends at the regional and global scales due to regional disparities of natural resources (Easterling et al., 1997; Crowley, 2000; Blandford et al., 2008; Li et al., 2016; Ozturk et al., 2017). Besides, regional climatic variations can increase the occurrence of droughts and floods due to the uneven availability of water (Yang and Lau, 2004). Therefore, there is a growing demand for detecting regional oscillations of past trend, change, and variability in air temperature and precipitation resulting from global warming, this information is important for understanding the causes and the regional impacts of climate change on natural environment and ecosystems.

Researchers found that the warming at high-elevation sites was

* Corresponding author at: State Key Laboratory of Cryospheric Science, Northwest Institute of Eco-Environment and Resources, Chinese Academy of Sciences, Lanzhou, 730000, China.
E-mail address: shichang.kang@lzb.ac.cn (S. Kang).

https://doi.org/10.1016/j.atmosres.2017.12.007
Received 2 November 2017; Received in revised form 19 December 2017; Accepted 20 December 2017
Available online 22 December 2017
0169-8095/

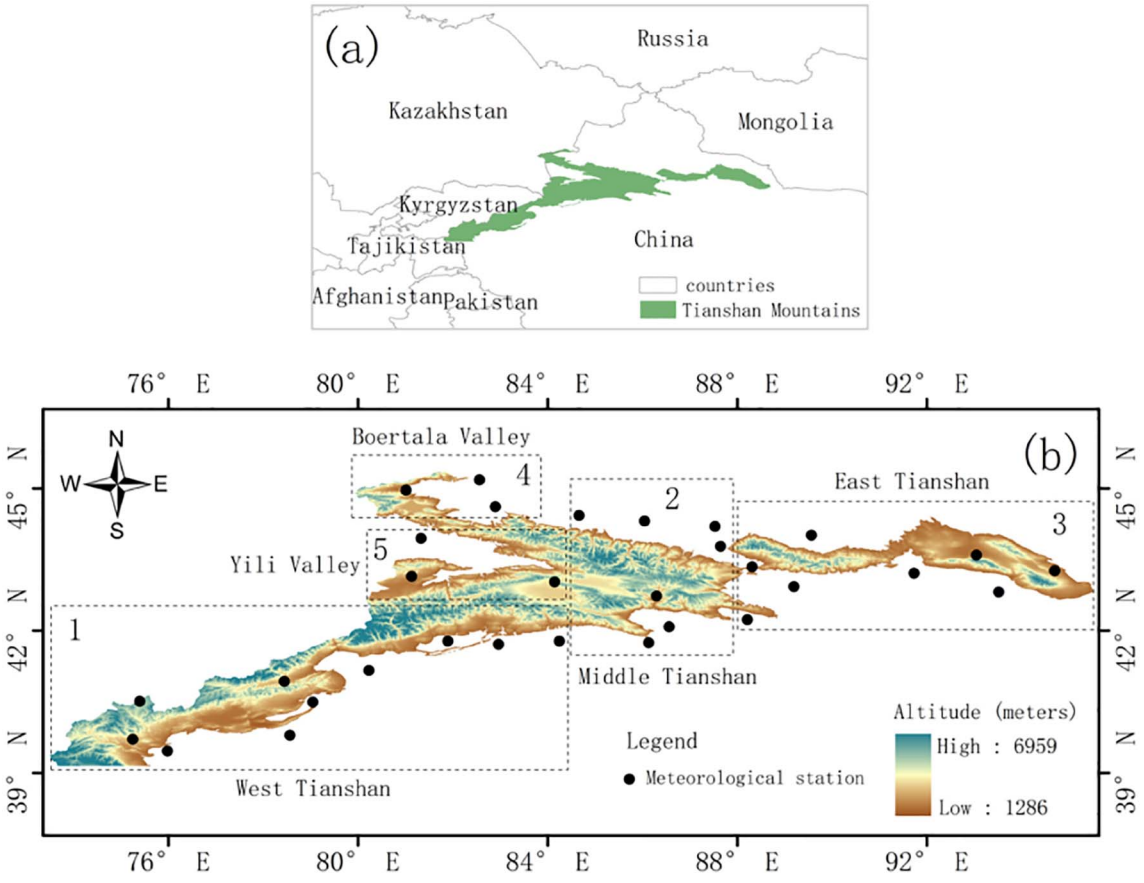

Fig. 1. Locations of Tian Shan Mountains and selected meteorological stations.

more pronounced than at low-elevations, recent concern about regional changes of temperature and precipitation have focused attention on high-elevation areas and mountains (Blandford et al., 2008; You et al., 2010; Holden and Rose, 2011; Wang et al., 2013; Deng et al., 2015; Guo and Li, 2015; Guo et al., 2016). The Tianshan Mountains are the largest mountain systems in Central Asia which is a semi-arid and arid region (Chen et al., 2016). As great northern peripheral mountains, the Tianshan Mountains play an important role of determining the climatic processes in the global and regional climate systems of Central Asia (Aizen et al., 1995; Aizen, 1997). Due to the long distance to the surrounding oceans causes lower precipitation and a dry climate in Central Asia, glaciers and snow of the Tianshan Mountains are important water resources in Central Asia, and are affected by various effects in changes of temperature and precipitation (Ye et al., 2005; Sorg et al., 2012; Chen et al., 2015; Deng et al., 2015; Xu et al., 2017a, 2017b). Global warming has accelerated the hydrological cycle (Brutsaert and Parlange, 1998; Gao et al., 2007; Yang et al., 2011). The changes of air temperature and precipitation in the Tianshan Mountains not only affected the changes of glaciers, but also influenced on hydrological systems which provide supplies for approximately 50 million people in Kyrgyzstan, Kazakhstan, Uzbekistan, northern Tajikistan, and the Xinjiang Province of China and support lowland agriculture, urban areas, and industries within those regions (Chen et al., 2008; Sorg et al., 2012; Ling et al., 2013a, 2013b; Xu, 2017). The Tianshan Mountains is highly vulnerable to changes in climate. The changes in temperature and precipitation of the mountain significantly affect the surrounding lowlands.

Meteorological station observations is an important and reliable data source for exploring climate change in alpine regions, these data can not only reveal climatic conditions, but also facilitate for the validation of climate models and accurate simulation of future climate change. Based on observation data, previous studies indicated that air temperature has exhibited a rising trend, and precipitation has increased in Central Asia (Lioubimtseva et al., 2005; Li et al., 2015). Inner Asia and northern China have experienced simultaneously a warming trend and decreasing precipitation over the past 40 years (Piao et al., 2010). As a main area of Central Asia, the air temperature in the arid region of northwest China demonstrated a significant rising trend by a rate of 0.33–0.34 °C/10a since 1960s, and the precipitation had a significantly increasing trend, at a rate of 0.61 mm/a (Sun and Yin, 2010; Li et al., 2016). Some studies also showed that both the temperature and precipitation display increasing tendency during past several decades in the Tianshan Mountains (Xi et al., 2005; Wang et al., 2011). In previous studies, the Tianshan Mountains were included or results were only reported roughly on whole mountain. However, the Tianshan Mountains are a huge region, the air temperature and precipitation has typical characteristics of multi-scale in space and nonlinearity. The air temperature and precipitation in different sub-regions and elevations of the Tianshan Mountains were not investigated systematically.

In this study, the objective is to understand the tempo-spatial characteristics of air temperature and precipitation during 1961–2016 over the Tianshan Mountains, its sub-division and different elevations using non-parametric methods. The mutations, significant periodic changes, large scale atmospheric circulation and elevation dependence of trends in air temperature and precipitation were discussed. The results will provide useful information for assessment of the impacts of

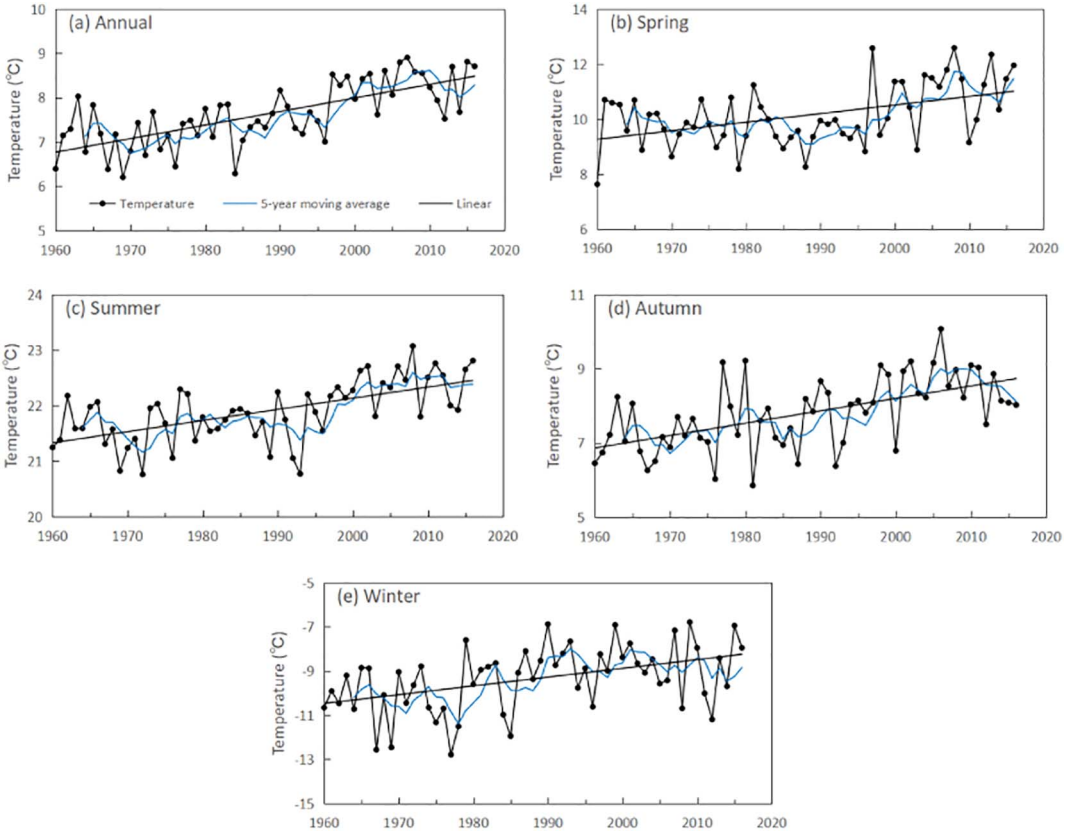

Fig. 2. Variations of annual and seasonal mean air temperature in the Tianshan Mountains during 1960–2016.

climate change and for improving the planning and management of the ecological environment in this region. In Sections 2 and 3, a brief description of study area, dataset and methods are provided, respectively. Section 4 presents the results of climate change in the Tianshan Mountains, different sub-regions and elevations. The discussion and conclusions are given in Sections 5 and 6, respectively.

2. Study area and data

2.1. Description of the study area

The Tianshan Mountains, which are located in the hinterland of Eurasia, stretch 2000 km from west to east and cover 800,000 km^2 (Aizen, 1997). In this study, we investigated the region between 39° and 46°N and 69° and 95°E (Fig. 1). The climatic regimes are determined by the interactions between the southwestern branch of the Siberian anticyclonic circulation and cyclonic activity from the west, and the water vapor transport system is mainly controlled by westerly circulation (Qi and Kulmatov, 2008). The Tianshan Mountains are far from the oceans, the region is characterized by a typical continental climate with low precipitation and large diurnal temperature variations. The orientation and height of the Tian Shan Mountains have a significant effect on weather patterns and the distribution of precipitation. The latest investigation has shown that there are 7934 glaciers in the Tianshan Mountains of China, the total area and volume of glaciers are 7179.77 km^2 and 707.95 km^3 (Liu et al., 2015). The study area is divided into five sub-regions in this study (Fig. 1(b)): West Tianshan (Region 1), Middle Tianshan (Region 2), East Tianshan (Region 3), Boertala Vally (Region 4) and Yili Valley (Region 5).

2.2. Dataset

The meteorological dataset was provided by the Climate Data Center of the China Meteorological Administration (CMA) (http://ncc.cma.gov.cn). There are 31 meteorological stations with least 50-year records by 2016 (1960–2016). The detailed information from the stations is shown in Fig. 1 and Table 1. The data records included monthly air temperature and precipitation. The preliminary quality control for the conventional near surface meteorological observation data sets has been done by CMA. It has also been popularly used in the study of climate changes in China (Zhang et al., 2016; Gao et al., 2017). The missing data were interpolated using the nearest available data by linear interpolation. The data were assessed by plotting the time series and inspecting the possible errors and uncertainties (Kousari et al., 2013). In order to maintain the spatial consistence as well as temporal homogeneity of temperature and precipitation records, the 31 sites were subject to strict quality control procedures by applying the RClimDex software package (http://etccdi.pacificclimate.org/software.shtml) to detect, and adjust for, multiple change points that could exist in the data series. Finally, all stations in the study area during the period 1960–2016 are retained. The sub-regions are listed in the last column of Table 1. The elevations of stations used in this study vary over a wide range, from 34.5 m (Tlulufan in East Tianshan) to 4801 m (Tuergate in West Tianshan). There are 6 stations at elevations below 500 m, 8 stations between 500 m and 1000 m, 9 stations between 1000 m and 1500 m, 5 stations between 1000 m and 1500 m and 3 stations above 2000 m (Table 1). The four seasons are defined as spring (March to May), summer (June to August), autumn (September to November) and winter (December to February).

To investigate changes in large scale atmospheric circulation,

Table 1
The information of meteorological stations in study area and sub-regions.

ID	Station name	Latitude (°)	Longitude (°)	Elevation (m)	Region
51709	Kashi (KS)	39.47	75.98	1289.4	(1) West Tianshan
51705	Wuqia (WQ)	39.72	75.25	2175.7	
51716	Bachu (BC)	39.80	78.57	1116.5	
51720	Keping (KP)	40.50	79.05	1161.8	
51701	Tuergate (TG)	40.52	75.40	3504.4	
51711	Aheqi (AHQ)	40.93	78.45	1984.9	
51628	Akesu (AKS)	41.17	80.23	1103.8	
51644	Chuche (KC)	41.72	82.97	1081.9	
51633	Baicheng (BC)	41.78	81.90	1229.2	
51642	Luntai (LT)	41.78	84.25	976.1	
51656	Kuerle (KEL)	41.75	86.13	931.5	(2) Middle Tianshan
51567	Yanqi (YQ)	42.08	86.57	1055.3	
51467	Baluntai (BLT)	42.73	86.30	1739.0	
51463	Urumqi (UQ)	43.78	87.65	935.0	
51365	Caijiahu (CJH)	44.20	87.53	440.5	
51356	Shihezi (SHZ)	44.32	86.05	442.9	
51346	Wusu (WS)	44.43	84.67	478.7	
51526	Kumishi (KMS)	42.23	88.22	922.4	(3) East Tianshan
52203	Hami (HM)	42.82	93.52	737.2	
51573	Tulufan (TLF)	42.93	89.20	34.5	
51495	Qijiaojing (QJJ)	43.22	91.73	721.4	
52118	Yiwu (YW)	43.27	94.70	1728.6	
51477	Dabancheng (DBC)	43.35	88.32	1103.5	
52101	Balikun (BLK)	43.60	93.05	1677.2	
51379	Qitai (QT)	44.02	89.57	793.5	
51334	Jinghe (JH)	44.62	82.90	320.1	(4) Boertala Valley
51330	Wenquan (WQ)	44.97	81.02	1357.8	
51232	Alashankou (ALSK)	45.18	82.57	336.1	
51542	Zhaosu (ZS)	43.15	81.13	1851.0	(5) Yili Valley
51437	Yining (YN)	43.95	81.33	662.5	
51431	Bayinbuluke (BYBLK)	43.03	84.15	2458.0	

monthly mean geopotential height and wind fields at 500 hPa derived from National Centers for Environmental Prediction/National Center for Atmospheric Research (NCEP/NCAR) reanalysis data during 1960–2016 were also analysed. The dataset is available at http://www.cdc.noaa.gov.

Table 2
Mann-Kendall test on monotonic trend for air temperature in the Tianshan Mountains during 1960–2016.

	Z_c	β	H_0	Cv
Annual	5.71[b]	0.032	R	0.09
Spring	2.77[a]	0.027	R	0.11
Summer	4.62[b]	0.022	R	0.03
Autumn	3.74[b]	0.032	R	0.12
Winter	2.80[b]	0.033	R	0.16

R: rejected; A: accepted.
[a] 95% confidence level.
[b] 99% confidence level.

3. Methods

3.1. Mann-Kendall monotonic trend test

Mann-Kendall monotonic test was applied to detect trends in hypothesis testing of hydro-meteorological time series which is without specifying whether the trend is linear or nonlinear (Kendall and Stuart, 1973). The null hypothesis (H_0) assumes that there is no significant increased or decreased trend in the time series, while the time series has a significant variation trend based on the alternative hypothesis (Li et al., 2012a, 2012b; Ling et al., 2013a). The test statistic (S) is described by the following equation:

$$S = \sum_{i=1}^{n-1} \sum_{j=i+1}^{n} \mathrm{sgn}(x_j - x_i) \tag{1}$$

x_i is a time-series from $i = 1, 2, 3 \ldots n-1$, and x_j is another time-series from $j = i+1,., n$, x_j is greater than x_i, n is the data set record length. Each point x_i is used as a reference point of x_j, the results are recorded as sgn (θ):

$$\mathrm{sgn}(\theta) = \begin{cases} 1, \theta > 0 \\ 0, \theta = 0 \\ -1, \theta < 0 \end{cases} \tag{2}$$

If the data set is identically and independently distributed, then the mean of S is zero and the variance of S is as follow:

$$Var[S] = \left[n(n-1)(2n+5) - \sum_t t(t-1)(2t+5) \right] / 18 \tag{3}$$

where n is the length of the data set, t is the extent of any given time, and represents the sum over all ties. Then, the test statistic is given as Z_c. For a long time-series, statistical value S can be transformed into Z_c, the equation is as follows:

$$Z_c = \begin{cases} \frac{S-1}{\sqrt{\mathrm{var}(S)}} S > 0 \\ 0, S = 0 \\ \frac{S+1}{\sqrt{\mathrm{var}(S)}}, S < 0 \end{cases} \tag{4}$$

When Z_c is $-1.96 \le Z_c \le 1.96$, the null hypothesis (H_0) is accepted, which indicates that there is no obvious trend. The trend is significant at the 95% confidence level if $|Z| > 1.96$ and at the 99% confidence level if $|Z_c| > 2.58$. A positive Z_c indicates that the sequence has an increased trend, while a negative Z_c reflects a declining trend (Kendall and Stuart, 1973). Besides identifying whether a trend exists, the Kendall inclination is usually used to detect the monotonic trend. The magnitude of trend can be defined as follows:

$$\beta = \mathrm{Media}\left(\frac{x_i - x_j}{i - j} \right), \forall j < i \tag{5}$$

where $1 < j < i < n$, positive β indicates an increased trend, and negative β indicates a decreased trend.

3.2. Abrupt change test

Abrupt change denotes a fast transition from one state to another (Berger and Labeyrie, 1985). It occurs when the climate system is

Table 3
Decadal statistics of annual and seasonal air temperatures in the Tianshan Mountains (°C).

	1960–1969	1970–1979	1980–1989	1990–1999	2000–2010	2011–2016	1960–1990	1970–2000	1980–2010	1990–2016
Annual	7.04	7.11	7.36	7.79	8.39	8.22	7.20	7.44	7.86	8.13
Spring	9.86	9.55	9.58	9.90	11.02	11.22	9.67	9.73	10.20	10.65
Summer	21.57	21.60	21.66	21.81	22.43	22.45	21.63	21.71	21.98	22.20
Autumn	7.04	7.40	7.45	8.04	8.68	8.27	7.34	7.60	8.08	9.35
Winter	− 10.38	− 10.25	− 9.40	− 8.49	− 8.54	− 9.04	− 9.91	− 9.35	− 8.80	− 8.63

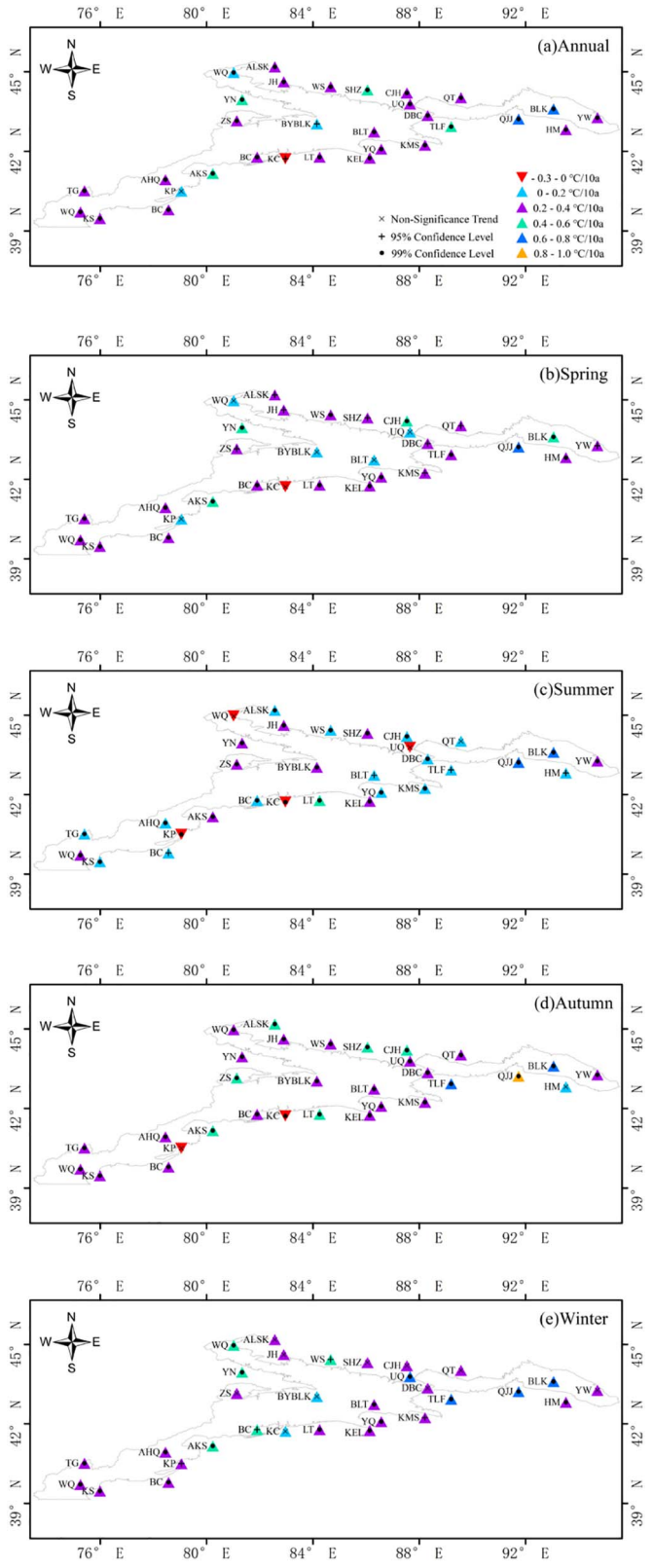

Fig. 3. Spatial trends for annual and seasonal air temperature during 1960–2016 over the Tianshan Mountains.

forced to cross a threshold. The Mann-Kendall abrupt change test is one of the most effective methods for testing abrupt time series changes which can clarify the start time of the mutation (Kendall, 1975; Hao et al., 2007). The method is used to analyze the change points of temperature and precipitation in this study. For time series X_n (n is the length of the data set), the order series (S_k) is given as follows:

$$S_k = \sum_{i=1}^{k} r_i, \ (k = 2, 3, 4, \ldots, n) \tag{6}$$

In which

$$r_i = \begin{cases} +1, & x_i > x_j \\ 0, & x_i \le x_j \end{cases}, \ (j = 1, 2, 3, \ldots, i) \tag{7}$$

where x_j and x_i are the sequential data values, and the statistic (UF_k) is defined as:

$$UF_k = \frac{[S_k - E(S_k)]}{\sqrt{Var(S_k)}}, \ (k = 1, 2, 3, \ldots, n) \tag{8}$$

where $UF_1 = 0$, $E(S_k)$ and $Var(S_k)$ are the average value and variance of S_k, which can be calculated by following equations:

$$E(S_k) = \frac{n(n+1)}{4} \tag{9}$$

$$Var(S_k) = \frac{n(n-1)(2n+5)}{72} \tag{10}$$

Then, the UB_k is calculated by repeating the above process in the order X_n, X_{n-1}, …, X_3, X_2, X_1 of the time series which makes $UB_k = UF_k$ ($UB_1 = 0$, $k = n, n-1, \ldots, 3, 2, 1$). The significance level is $p = 0.05$ in this study.

3.3. Morlet continuous wavelet transforms

The wavelet analysis was applicable in analysis of climate variables to detect the periodicity, phase change and periodic intensity during the time series (Torrence and Compo, 1998; Grinsted et al., 2004; Ling et al., 2013b). In this study, the periodicity is analysed by employing a chi-square test and detecting significant time sections from red noise standard spectra. The Morlet wavelet (ψt) represents a wave modulated by Gaussian function as following:

$$\psi(\bar{t}) = \pi^{-1/4} e^{ict} e^{-t^2/2} \tag{11}$$

where i is the unit of the imaginary number, t is the non-dimensional time parameter, and c is a constant number.

A discrete signal $f(t)$ with a Morlet wavelet (ψ_t) in the continuous wavelet transformation is expressed by:

$$W_f(a,b) = \frac{1}{a} \int_R f(t) \psi^* \left(\frac{t-b}{a} \right) dt \tag{12}$$

where $W_f(a, b)$ is the transformation coefficient, a and b are scale parameter and translation parameter. t is the time scale and ψ^* is the complex conjugate.

The main periodicity on different scales in time series is determined by wavelet variance which is expressed as:

$$Var(a) = \int_{-\infty}^{+\infty} |W_f(a,b)|^2 db \tag{13}$$

where, $Var(a)$ is the wavelet variance and time scale. The peak values of wavelet variance correspond to the main periods of different time scales (Torrence and Compo, 1998).

3.4. Climatic trend of lapse rate

The trend of elevation-dependent phenomenon was analysed by linear regression, the equation is expressed as:

$$Y = aX + b \tag{14}$$

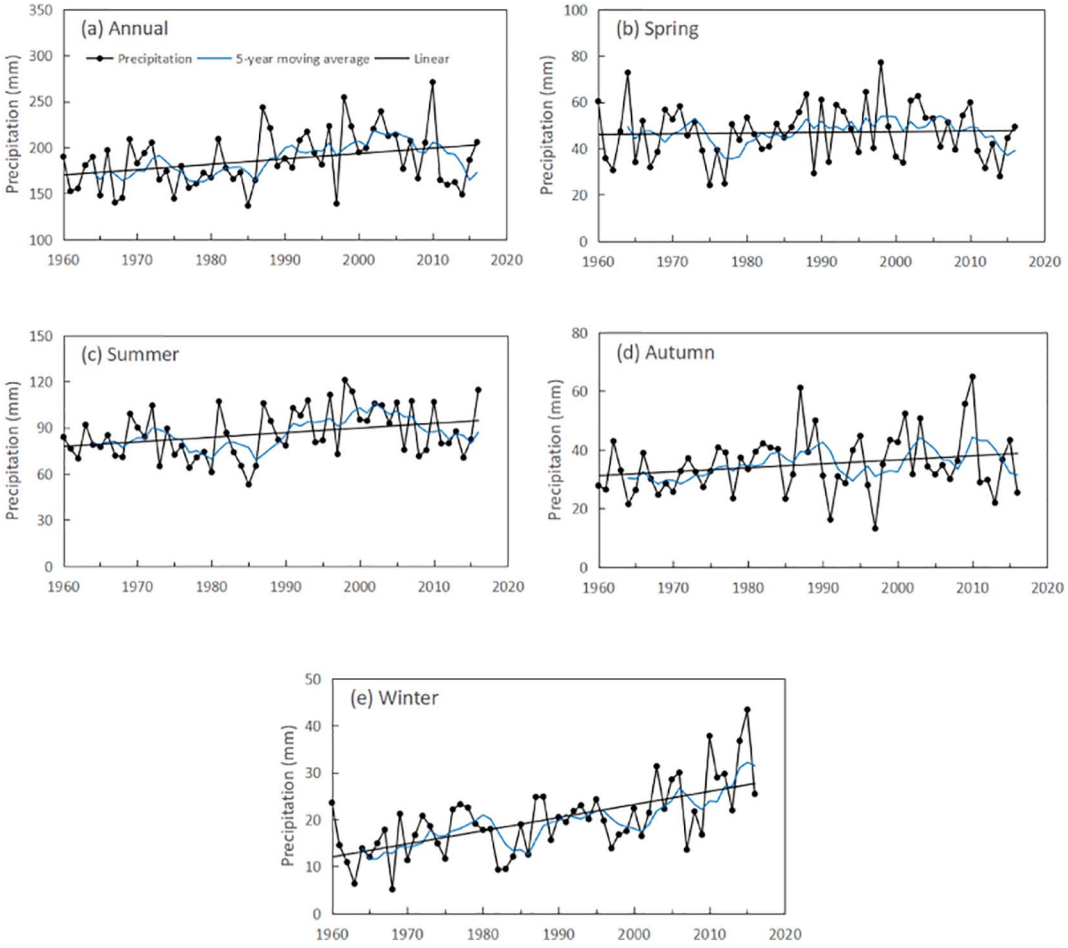

Fig. 4. Variations of annual and seasonal mean precipitation in the Tianshan Mountains during 1960–2016.

Table 4
Mann-Kendall test on monotonic trend for precipitation in the Tianshan Mountains during 1960–2016.

	Z_c	β	H_0	Cv
Annual	2.14[a]	0.582	R	0.16
Spring	0.39	0.041	A	0.25
Summer	2.17[a]	0.264	R	0.19
Autumn	1.63	0.114	A	0.29
Winter	4.61[b]	0.255	R	0.38

R: rejected; A: accepted.
[a] 95% confidence level.
[b] 99% confidence level.

where Y represents trend of meteorological variables; X is the elevation of each station; a and b are the regression slopes and intercepts, respectively.

4. Results and analysis

4.1. Temporal and spatial variations of temperature in the Tianshan Mountains

Fig. 2 shows the annual and seasonal variability of the temperature in the Tianshan Mountains. According to the Mann-Kendall monotonic trend test, significant positive trend in annual air temperature has been identified during 1960–2016, which reached a significance level of 0.01 ($|Zc| > 2.58$) (Table 2). The warming trend of annual air temperature over the last 57 years was 0.32 °C/10a which was much stronger than the global warming rate 0.19 °C/10a (Hansen et al., 2006). Annual air temperature has increased by around 1.82 °C during 1960–2016. The warmest year occurred in 2007 in the Tianshan Mountains. The air temperature also showed an significant increasing trend in summer, autumn and winter, whereas the increasing trend in spring was not statistically significant ($Zc = 1.66 < 1.96$) (Table 2). The air temperature increase for winter, spring, summer and autumn was 0.33 °C/10a, 0.27 °C/10a, 0.22 °C/10a and 0.32 °C/10a, respectively. The air

Table 5
Decadal statistics of annual and seasonal precipitation in the Tianshan Mountains (°C).

	1960–1969	1970–1979	1980–1989	1990–1999	2000–2010	2010–2016	1960–1990	1970–2000	1980–2010	1990–2016
Annual	170.81	173.60	183.95	200.67	209.76	171.37	176.50	186.35	198.50	197.86
Spring	46.04	42.98	47.35	52.85	49.64	39.09	45.96	47.37	49.94	48.49
Summer	80.66	79.38	79.56	96.91	94.27	85.87	79.82	85.61	90.38	93.38
Autumn	30.07	32.93	40.18	31.18	42.32	31.06	34.29	35.01	38.03	35.69
Winter	14.05	18.12	16.38	19.74	23.88	31.06	16.32	18.22	20.12	23.94

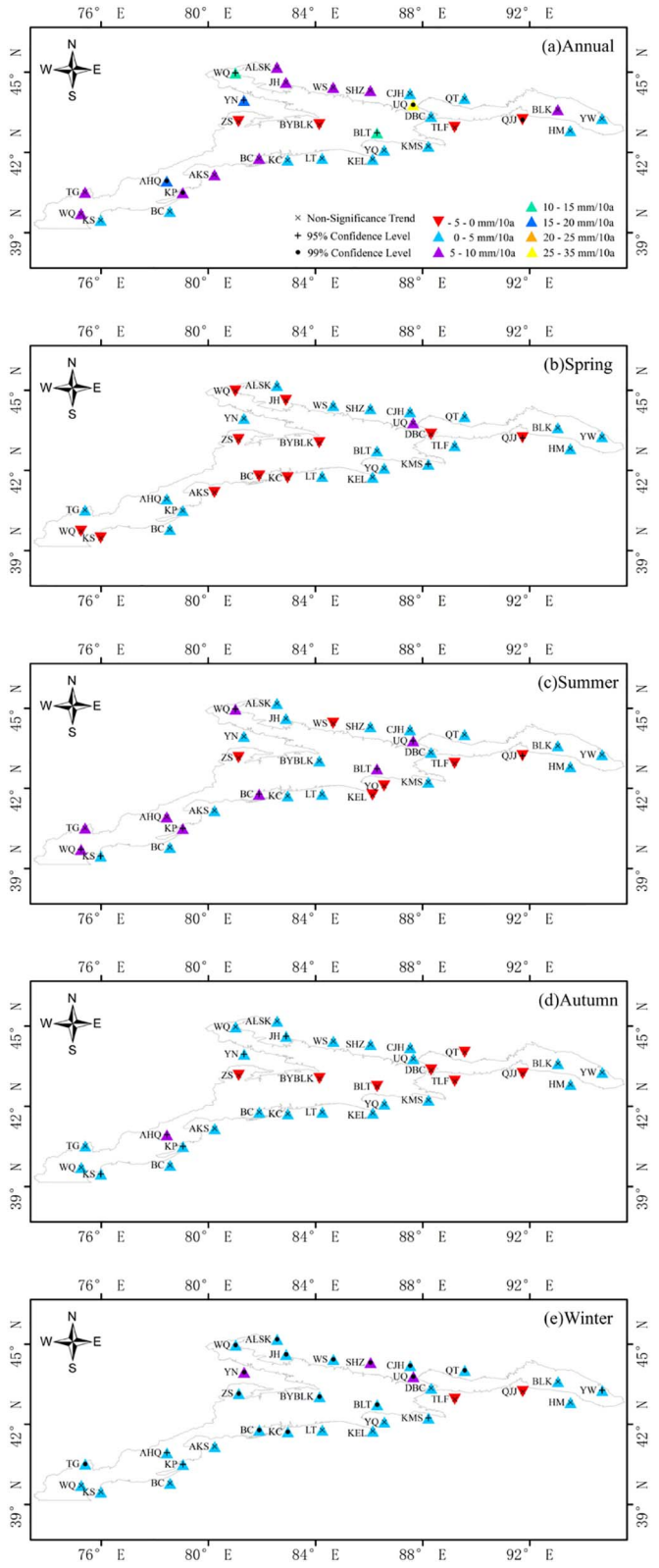

Fig. 5. Spatial trends for annual and seasonal precipitation during 1960–2016 over the Tianshan Mountains.

temperature in spring showed decreased trend during 1960–1995 (Fig. 2(b)). The rate of air temperature increased more significantly in winter than in the other three seasons. The least significant warming rate occurred in spring. Coefficients of variation (Cv) are used to measure the degree of dispersion of variables in time series. As shown in Table 2, the Cv of the air temperature was the largest in winter, which showed strong variability; the second one was Autumn. The Cv was the smallest in summer, showing weak variability. Table 3 shows statistics of annual and seasonal air temperatures in the Tianshan Mountains. The annual and seasonal air temperatures increased before 2010, with an exception in spring of the 1970s and 1980s and in winter of 2000s with a relatively lower temperature. Compared with the 1960s, annual air temperature in the 2000s has increased by 1.35 °C. However, winter temperature has increased by 1.84 °C. The annual and seasonal temperatures within 30-year average from 1990 to 2016 were highest within 30-year average from 1960 to 1990, 1970 to 2000 and 1980 to 2010. In contrast to other regions, the annual mean temperature rise rate in the Tianshan Mountains is relatively higher than Hengduan Mountains and Qilian Mountains of China, central Himalaya region and central Tibetan plateau (Du et al., 2000; Yang et al., 2006; Jia et al., 2008; Li et al., 2011). The Siberian High is a cold dry air mass formed in the Mongolian-Siberian region which has immense influence on the weather patterns in most parts of the Northern Hemisphere (Gong and Ho, 2002; Panagiotopoulos et al., 2005). The fluctuations of Siberian high intensity and air temperature in winter showed inverse phases in the mid-to-high latitude Asia and the arid region of northwest China, the correlation relationships were -0.58 and -0.715, respectively (Li et al., 2012a, 2012b). Besides, human activities may considerably modify the temperature pattern (Souleymane et al., 2011), excessive greenhouse gas emissions by human activities are generally regarded as the main cause of global warming (Mahlstein and Knutti, 2010). The carbon dioxide emissions in the past 20 years maintained a strongly increasing trend in China, and there was a positive correlation between greenhouse gas emission and winter temperature in the northwest region of China ($R = 0.51$) (Li et al., 2012a, 2012b). The fastest rapid warming also occurred in winter in the Tianshan Mountains. Therefore, both the weakening of Siberian High and increasing greenhouse gas emission contribute to warming trend in the Tianshan Mountains.

According to the Mann-Kendall monotonic trend test, Fig. 3 shows the annual and seasonal spatial distribution characteristics of the change rate of air temperature in the Tianshan Mountains. Except KC station, the annual air temperature at 30 stations showed a significant positive trend ($p < 0.05$). Owing to topographical complexity, the increasing rates of annual mean temperature were spatially varied ranging from 0.04 °C/10a (KP) to 0.78 °C/10a (QJJ) during 1960–2016. The warming rates in most of stations was between 0.20 °C/10a and 0.4 °C/10a, four stations varied from 0.4 °C/10a–0.6 °C/10a, and two stations varied from 0.6 °C/10a to 0.8 °C/10a. Although the annual air temperature at KC station had a downtrend, it was not statistically significant. As special geographic location of KC, the dramatic windy weather showed high frequency of occurrence and the wind speed increased in KC (Yang et al., 2015). In other hand, the increased vegetation cover increased the air humidity may have negative influence on processes of warming (Hu and Yao, 2008). The diversities of factors could form local microclimate in KC which led air temperature decrease. The temperature decreased obviously in summer and autumn and did not increased obviously in winter in KC which leads to the annual temperature deceased. The most pronounced warming of annual air temperature occurred at QJJ and BLK in the East Tianshan. In spring, the air temperature at KC showed decreasing trend with not significance. Although the increasing rates in spring range from 0.05 °C/10a (WQ, did not exceed the 95% confidence level) to 0.76 °C/10a (QJJ), the significance of some stations was not obviously. In summer, the air temperature of four stations (WQ, UQ, KC and KP) showed decreasing trend which did not exceed the 95% confidence level in WQ and UQ. In other stations, the warming tendencies were

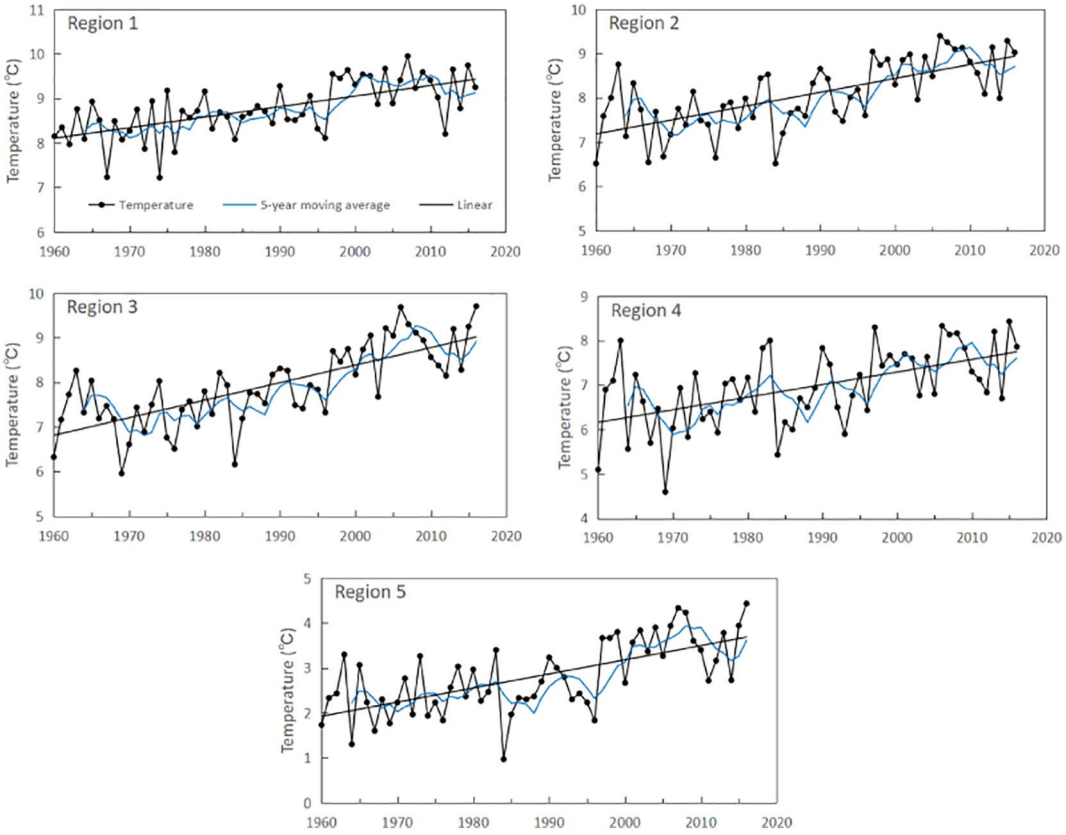

Fig. 6. Variations of annual mean air temperature in the sub-regions of the Tianshan Mountains during 1960–2016.

Table 6
Mann-Kendall test on monotonic trend for air temperature in the sub-regions of the Tianshan Mountains during 1960–2016.

	Z_c	β	H_0	Cv
Region 1	4.87[b]	0.023[a]	R	0.07
Region 2	5.47[b]	0.033	R	0.10
Region 3	6.06[b]	0.041	R	0.11
Region 4	4.23[b]	0.029	R	0.12
Region 5	5.19[b]	0.033	R	0.28

R: rejected; A: accepted.
[a] 95% confidence level.
[b] 99% confidence level.

from 0.04 °C/10a (QT, did not exceed the 95% confidence level) to 0.71 °C/10a (BLK). In autumn, except KC and KP (− 0.02 °C/10a, did not exceed the 95% confidence level) station, the warming rates ranged from 0.12 °C/10a (HM, did not exceed the 95% confidence level) to 0.89 °C/10a (QJJ). In winter, the warming rates ranged from 0.03 °C/10a (BYBLK, did not exceed the 95% confidence level) to 0.78 °C/10a (QJJ). The spatial variation of temperature showed different in annual and seasonal scale, it has significantly become warmer during the past decades in the Tianshan Mountains.

4.2. Temporal and spatial variations of precipitation in the Tianshan Mountains

The Mann-Kendall monotonic trends of annual and seasonal precipitation during 1960–2016 over the Tianshan Mountains are shown in Fig. 4. The annual precipitation has increased at a rate of 5.82 mm/10a in the Tianshan Mountains, which was lower than in the northwestern China with 6.1 mm/10a (Li et al., 2016). Annual mean precipitation has increased by around 33.2 mm from 1960 to 2016. The test statistic of Zc for the spring precipitation was 0.39 (Table 2), indicating that precipitation experienced a slight upward with a rate of 0.41 mm/10a. The increasing rates of precipitation in summer, autumn and winter were 2.64 mm/10a, 1.14 mm/10a and 2.55 mm/10a, respectively. In summer and winter, the increasing rates in other seasons exceeded the significance level of 0.05 ($|Zc| > 1.96$). The mean precipitation in spring, summer, autumn and winter is 46.89 mm, 86.27 mm, 35.01 mm and 19.86 mm in the Tianshan Mountains. From the magnitudes of increases in the relevant seasons, it can be seen that the increase of annual precipitation was mainly resulted from the precipitation increase in summer or rainy season. The Cv of precipitation in the regions were higher than those of temperature and ranged from 0.19 to 0.38, which indicated that precipitation changed more dramatically than temperature in the Tianshan Mountains. The Cv of precipitation in summer was the smallest, and the largest Cv was found in winter. Comparing to the 1960s, the annual precipitation in the 2000s has increased by 23% (38.95 mm) with the largest in winter (70%) (Table 3). Maximum precipitation in annual, autumn and winter occurred in the 2000s, and minimum precipitation occurred in the 1960s. Comparing to the 2000s, the precipitation decreased from 2011 to 2016. Before 2010, the maximum and minimum precipitation in spring and summer occurred in 1990s and 1970s, respectively. Compared with the period of 1960 to 1990 and 1970 to 2000, the 30-year annual mean precipitation during 1980–2010 has increased by 22.00 mm (12.5%) and 12.15 mm (6.5%), respectively. The annual precipitation increase rate was higher in the Tianshan Mountains than Hengduan Mountains and the Xinjiang autonomous region, but lower than Qilian Mountains and most areas of the Tibetan plateau (Du and Ma, 2004; Jia et al., 2008; Liu et al., 2009;

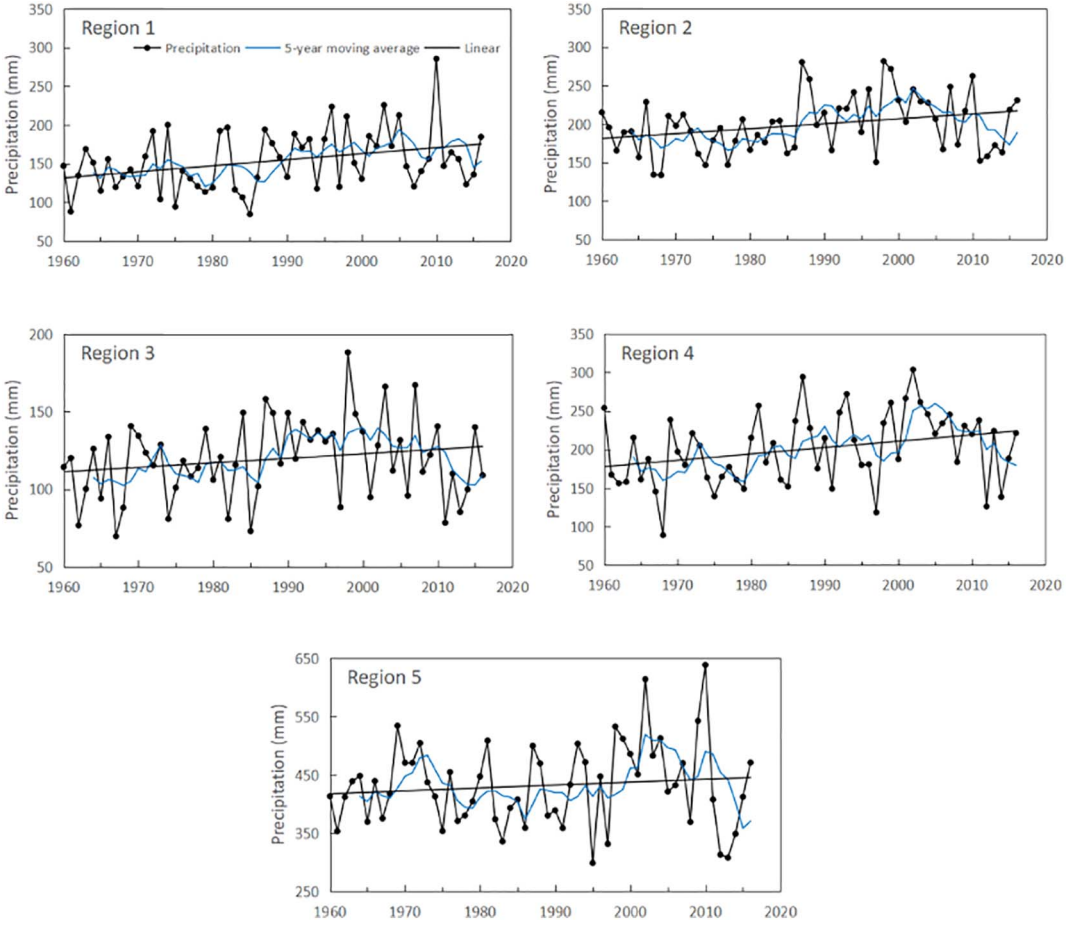

Fig. 7. Variations of annual mean precipitation in the sub-regions of the Tianshan Mountains during 1960–2016.

Table 7
Mann-Kendall test on monotonic trend for precipitation in the sub-regions of the Tianshan Mountains during 1960–2016.

	Z_c	β	H_0	Cv
Region 1	2.17[a]	0.661	R	0.25
Region 2	2.13[a]	0.642	R	0.19
Region 3	1.16	0.264	A	0.21
Region 4	2.22[a]	0.807	R	0.23
Region 5	0.71[b]	0.458	A	0.17

R: rejected; A: accepted.
[a] 95% confidence level.
[b] 99% confidence level.

Li et al., 2011). Previous studies indicated that the Tibetan Plateau affects the atmospheric circulation, it will cause a moisture increase from the Caspian Sea into the Tianshan Mountains, and precipitation may increase (Bothe et al., 2012; Chen et al., 2014). In large scale, the main reasons for the wetting trend in the Tianshan Mountains were probably the strengthening of the North America Subtropical High and West Pacific Subtropical High (Li et al., 2016; Yao et al., 2016). The increase of North America Subtropical High enhanced water vapor transported from the Atlantic to Central Asia, the precipitation increases significantly by westward flowing wind. The stronger West Pacific Subtropical High leads to more water vapor transport to the Tianshan Mountains (Tables 4 and 5).

Fig. 5 shows the spatial trend of precipitation for annual, spring, summer, autumn and winter in the Tianshan Mountains by Mann-Kendall monotonic test. Three stations (ZS, BYBLK and TLF) in annual precipitation showed a downward trend with non-significant trends, the decreasing rate were − 3.56 mm/10a, − 0.97 mm/10a and − 0.91 mm/10. The precipitation in QJJ decreased significantly with a rate of − 4.99 mm/10a. Although a large number of stations in annual precipitation had a positive change, there were 20 stations (64%) of them showed a non-significant upward trend. The increasing rates of annual precipitation ranged from 0.41 mm/10a (YQ) to 25.38 mm10/a (UQ). In spring, although 20 stations exhibited increasing trends, most of them did not pass the 95% confidence level with rate of 0–5 mm/a. 11 stations exhibited decreasing trends, but no significant trend was found for most of them, seven of them are located in the West Tianshan (WQ, KS, AKS, BC and KC) and East Tianshan (DBC and QJJ), respectively, and four was located in Yili valley (ZS and BYBLK) and Boertala Valley (JH and WQ). In summer, 5 stations exhibited decreasing trends with non-significant trend from Yili Valley to East Tianshan. The increasing trends in summer were most evident and the increasing amplitudes were also large, ranging from 0.86 mm/10a (SHZ) to 9.53 mm/10a (BLT). In autumn, 78% of stations showed increasing trend in precipitation, most of them did not pass the 95% confidence level with test, accounting for 80% of the total number of stations, seven stations displayed non-significant decreasing trends, and these stations were located in the Yili valley (ZS and BYBLK), Central Tianshan (BLT) and East Tianshan (DBC, QT, TLF and QJJ). In winter, only TLF and QJJ showed decreasing with non-significant trend. In the north part of the Tianshan Mountains, the most of stations showed an increasing trend in

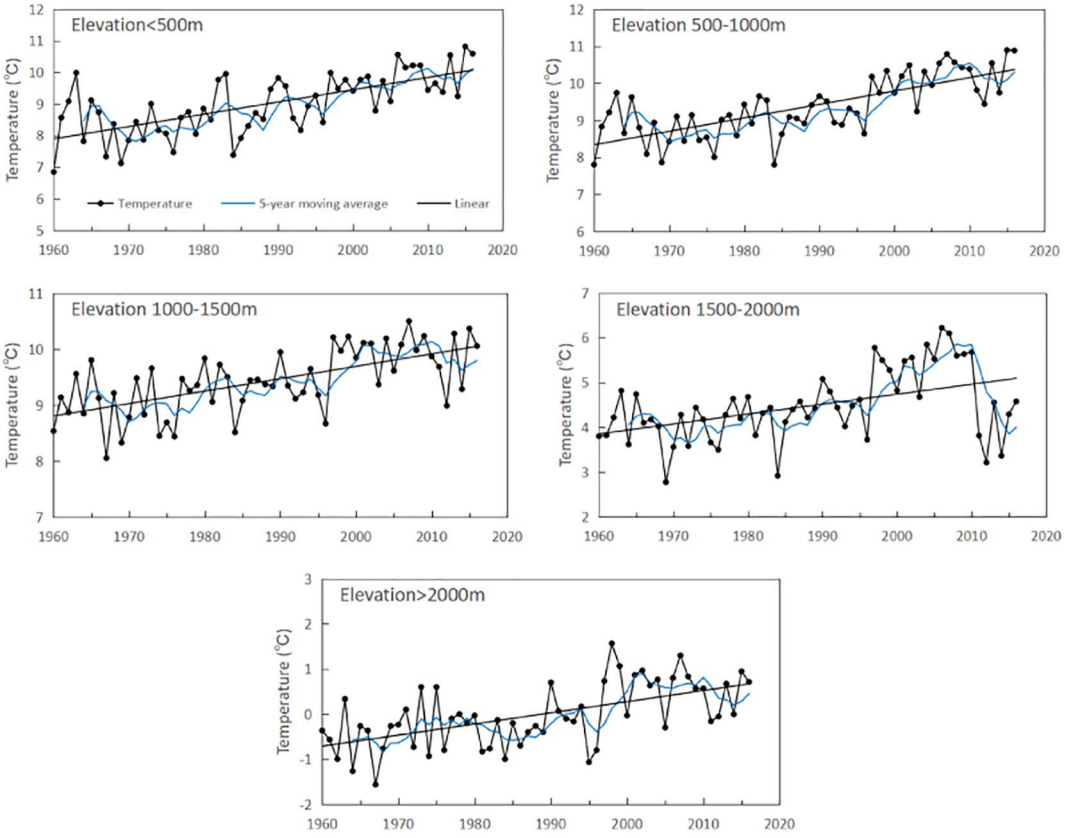

Fig. 8. Variations of annual mean air temperature in the different elevations of the Tianshan Mountains during 1960–2016.

Table 8
Mann-Kendall test on monotonic trend for air temperature in the different elevations of the Tianshan Mountains during 1960–2016.

	Z_c	β	H_0	Cv
< 500 m	5.31[b]	0.042[a]	R	0.10
500–1000 m	6.08[b]	0.038	R	0.08
1000–1500 m	4.78[b]	0.023	R	0.06
1500–2000 m	3.99[b]	0.025	R	0.18
> 2000 m	4.42[b]	0.024	R	10.66

R: rejected; A: accepted.
[a] 95% confidence level.
[b] 99% confidence level.

winter, which reached a significance level of 0.01 ($|Zc| > 2.58$). In the West Tianshan and East Tianshan, the precipitation did not pass the 95% confidence level with Mann-Kendall monotonic test in winter. Overall, the Tianshan Mountains has become wetter during the past decades.

4.3. *Trends of mean annual temperature and precipitation in the sub-regions of the Tianshan Mountains*

Fig. 6 shows the change processes of the annual mean air temperature for the five sub-regions in the Tianshan Mountains during 1960–216. The air temperature fluctuated differently in processes but overall increased in five sub-regions, the Mann-Kendall monotonic trend test statistics reached a significance level of 0.01 ($|Zc| > 2.58$) (Table 6). The temperatures of the Region 3 in the East Tianshan increased most rapidly at rates of 0.41 °C/10a. The second highest rates were observed on the Region 2 at 0.33 °C/10 in the Middle Tianshan. The observed rate of increase in temperature was lowest in the Region 1 area of the West Tianshan at 0.23 °C/10a. In the Boertala Vally and Yili Valley, the temperature increased by 0.29 °C/10a and 0.33 °C/10a, respectively. The regional warming characteristics were obvious in the Tianshan Mountains, and the rates increased gradually from west to east and were higher on the north slope than on the south slope. The temperature of the Region 1, 2, 3 and 4 varied weakly during 1960–2016 (Table 6). The highest variability was observed in the Region 5, which indicates that the fluctuations were more drastic Yili Valley than in other regions. The degree of fluctuation was more intensive on the north slope of the Tianshan Mountains than on the south slope, whereas degree of fluctuation in the West Tianshan was lower than that in the East Tianshan.

The monotonic trends of annual precipitation during 1961–2016 in the sub-regions of the Tianshan Mountains are shown in Fig. 7. The annual precipitation showed different patterns of fluctuation. The annual precipitation had significant increasing trends at a test level of 0.05 ($-1.96 \le Zc \le 1.96$) in the Region 1 (West Tianshan), Region 2 (Middle Tianshan) and Region 4 (Boertala Vally), and the annual precipitation did not increased significantly in the Region 3 (East Tianshan) and Region 5 (Yili Vally) (Table 7). The annual precipitation showed increases of 6.61 mm/10a and 6.42 mm/10a in the Region 1 (West Tianshan) and Region 2 (Middle Tianshan), respectively. The increasing magnitudes were highest in the Region 4 (Boertala Vally) and lowest in the Region 3 (East Tianshan). As can be seen in Table 7, the increased rates of annual on the north slope (Region 4 and 5) were higher than that on the south slope overall (Region 1). The precipitation change rate increased from the low-value area (Region 3) in the East Tianshan to the high-value area (UQ) in the Middle Tianshan (Region 2), and the rate then decreased in the West Tianshan, although the

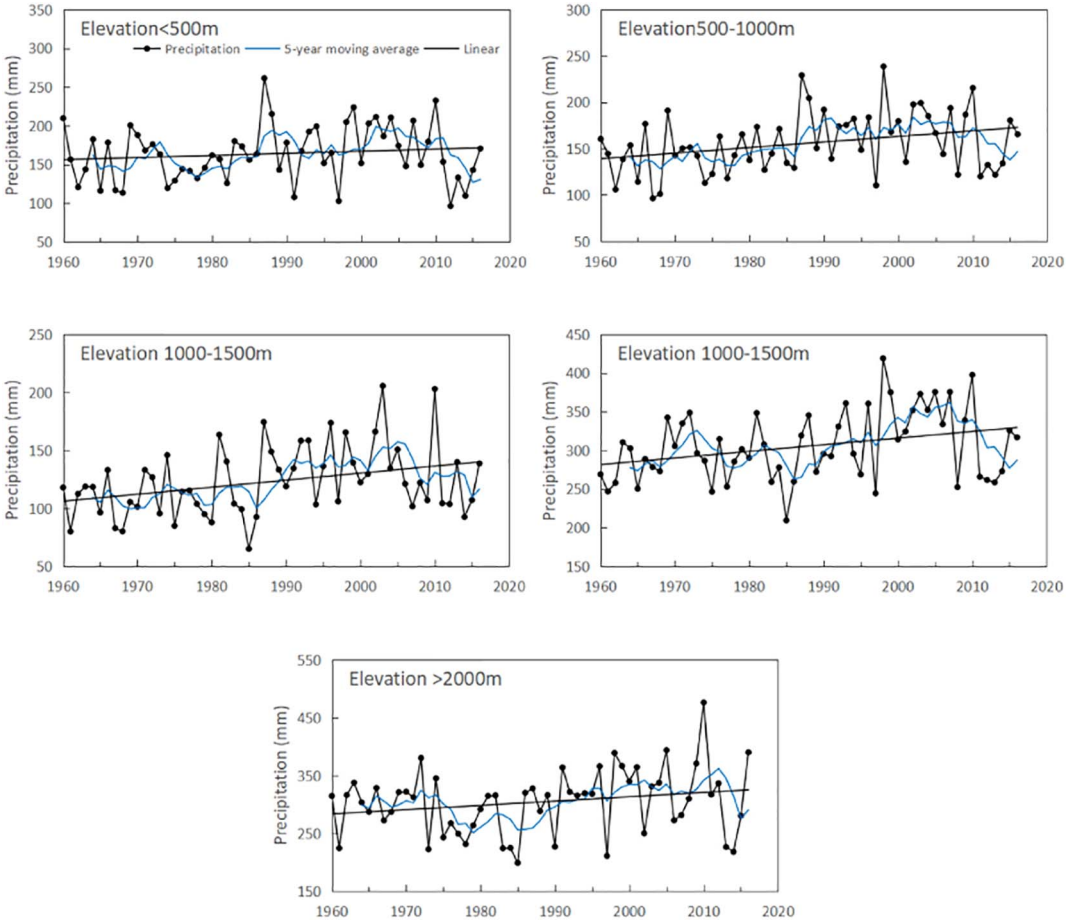

Fig. 9. Variations of annual mean precipitation in the different elevations of the Tianshan Mountains during 1960–2016.

Table 9
Mann-Kendall test on monotonic trend for precipitation in the different elevations of the Tianshan Mountains during 1960–2016.

	Zc	β	H_0	Cv
< 500 m	0.10	0.345	R	0.21
500–1000 m	2.24[a]	0.671	R	0.21
1000–1500 m	2.43[a]	0.513	R	0.24
1500–2000 m	2.39[a]	0.922	R	0.15
> 2000 m	1.70[b]	0.657	R	0.18

R: rejected; A: accepted.
[a] 95% confidence level.
[b] 99% confidence level.

value was higher than that in the eastern part. The Cv in annual precipitation were higher than air temperature and ranged from 0.17 to 0.25, which indicated that precipitation changed more dramatically than air temperature in the Tianshan Mountains. The Cv in precipitation on the Region 5 were the smallest (0.17), and the largest coefficients were found in the Region 1 (0.25). Compared with temperature, the Cv in annual precipitation were higher on the west part than on the east part and higher in the south slope. To a certain extent, the obvious changes of Cv in annual precipitation led to larger changes of air temperature (Tables 6 and 7). However, the obvious larger fluctuation of precipitation in the Region 1 caused the air temperature to stabilize, the state was opposite in the Region 5 which indicated that the changes of air temperature was more sensitive to changes of precipitation in the Yili Valley.

4.4. Trends of mean annual temperature and precipitation in the different elevations of the Tianshan Mountains

Fig. 8 shows the inter-annual variations of air temperature during 1960–2016 in the different elevations of the Tianshan Mountains. The fluctuations of air temperature showed differently in different elevations. Our analysis shows that a significant warming trend was found for all the elevations tested, with the greatest warming below 500 m (0.42 °C/10a), and the weakest in the elevation of 1000–1500 m (0.23 °C/10a) (Table 2). After a decrease in the 1960s, the annual air temperature started to fluctuate and increased in all elevations. Annual air temperature rose in the 1970s, slightly increased during 1970–1980, decreased after 1980, but slightly increased after 1985. As can be seen, the obvious increased after 1995 in all elevations. In the elevation of 500–1000 m and 1000–1500 m, the air temperature was more stable. The higher variability was observed in the elevation of 1500–2000 m and above 2000 m, which indicates that the fluctuations were more drastic than in other elevations (Table 8).

The Mann-Kendall trend test results for long-term precipitation in the Tianshan Mountains are shown in Fig. 9 and Table 9. The annual precipitation in the different elevations showed increasing trends in the study period. The annual precipitation had significant increasing trends at a test level of 0.05 ($-1.96 \leq Z_c \leq 1.96$) in the elevation of 500 m–1000 m, 1000 m–1500 m and 1500 m–2000 m, and the precipitation did increased significantly in other elevations. The increasing magnitudes were highest in the elevation of 1500 m–2000 m (9.22 mm/10a) and lowest in the elevation of below 500 m (3.45 mm/10a). The increased rates of precipitation were 6.71 mm/10a,

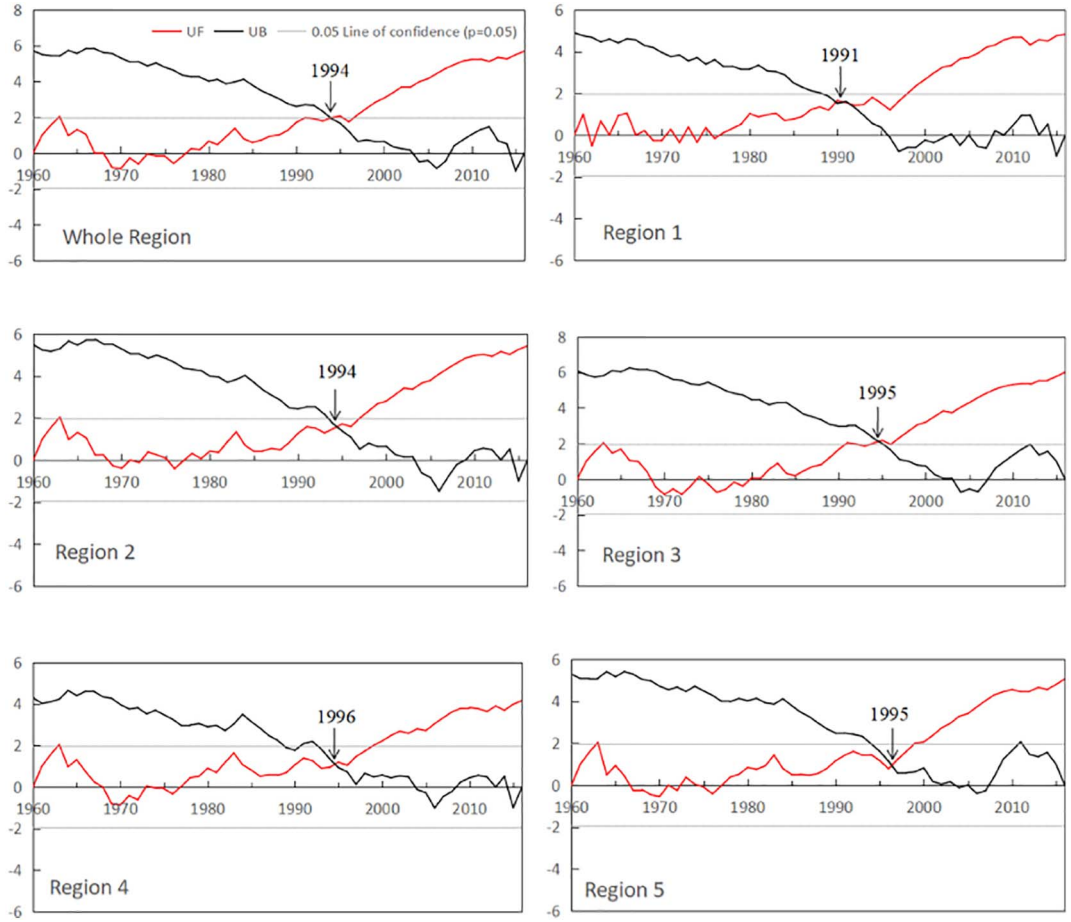

Fig. 10. Abrupt change of annual air temperature in the Tianshan Mountains and sub-regions during 1960–2016.

5.13 mm/10 and 6.57 mm/10a in 500 m–1000 m, 1000 m–1500 m and above 2000 m, respectively. The Cv in precipitation were higher below 1500 m. Below 500 m, the annual precipitation increased during 1960–1973, decreased during 1973–1980, and increased after 1980. In the elevation of 500 m–1000 m and 1000 m–1500 m, the annual precipitation was relative more stable during 1960–1985, and then showed obviously increased after 1985. In the elevation of 1000 m–1500 m, the annual precipitation increased during 1960–1973, and decreased during 1973–1985, then increased after 1985. The annual precipitation decreased during 1960–1980 and then exhibited a variation with "saddle shape" during 1980s, it was more stable after 1900. The changes of annual precipitation were more complicated than changes of air temperature in the different elevations of the Tianshan Mountains.

5. Discussions

5.1. The mutations of annual air temperature and precipitation over the Tianshan Mountains

The abrupt change of climate denotes climate transition from one stable state to another, it occurred when the climate system was forced to cross a threshold, triggering a transition to a new state at a rate determined by the climate system (Berger and Labeyrie, 1985; Matyasovszky, 2011). The Mann-Kendall abrupt change test was used to monitor the change points of climate in the different regions. Fig. 10 shows the temporal processes of the statistics UF and UB curves obtained from the Mann-Kendall test for sub-regions, the confidence interval was set as 95% (corresponding to the statistically significance level $\alpha = 0.05$). As the intersections of UF and UB curves in Fig. 5 were all inside of the confidence interval, the abrupt change of air temperature in the Tianshan Mountains was observed in 1994, and it occurred in 1991 for Region 1 (West Tianshan). The Region 2 occurred in 1994. The Region 3 and 5 occurred in 1995, and the Region 4 occurred in 1996. The mutation of air temperature occurred in 1990s in the Tianshan Mountains. UF curves represent the trend of the time series. As can be seen, the air temperature in the Region 1 fluctuated obviously before 1975, after that the air temperature experienced a significant upward trend until 2016. Except Region 1, the air temperature exhibited a variation with "saddle shape" during 1960–1970. A continuous rising process occurred since late 1970s in the Region 1, Region 2, Region 4 and Region 5. In the Region 3, the increasing trend since 1980.

The results of the abrupt change test of annual precipitation are shown in Fig. 11. The changes of annual precipitation were more complicated than changes of air temperature in the Tianshan Mountains. The abrupt change was observed in 1982 for whole Tianshan Mountains. The annual precipitation over whole region can be separated into three periods. The first period was from 1960 to the late 1980s with stable fluctuation, and second period was followed by a steep increase during 1980–2010, it decreased after 2010. The increasing trend did not exceed the 95% confidence level after late 1990s. The step change points occurred in 1987 and 1983 in the Region 1 and Region 2, respectively; in 2013 in the Region 3; in 1981 in the Region 4. There are two abrupt points in the Region 5, 1975 and 2012, respectively. The appearances of the change points in annual precipitation occurred earlier from the East Tianshan to West Tianshan. The

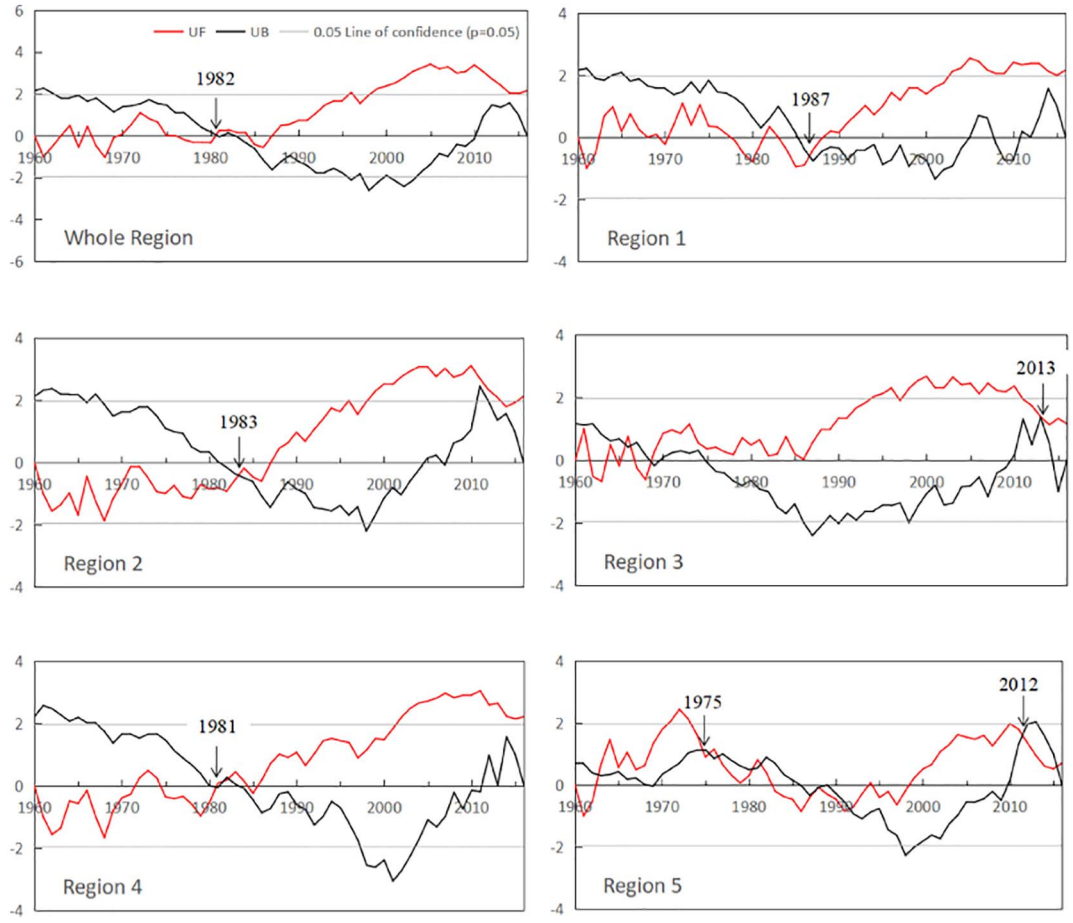

Fig. 11. Abrupt change of annual precipitation in the Tianshan Mountains and sub-regions during 1960–2016.

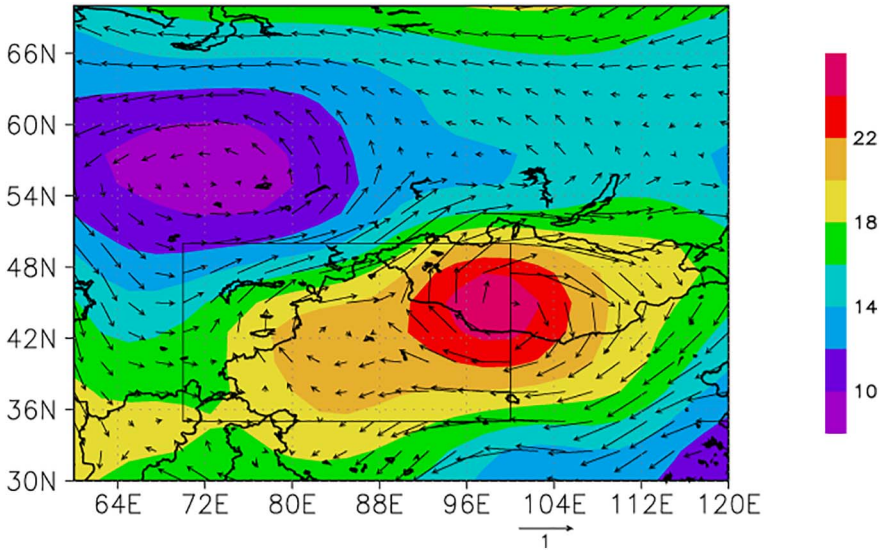

Fig. 12. Differences of geopotential height (shaded) and wind speed (vector) at 500 hPa between 1996–2016 and 1960–1995 (Black rectangle is the study area).

precipitation in the different sub-regions had different statuses in the different periods. In the Region 1 and 3, the fluctuations in annual precipitation began to increase continuously in 1990 and late 1980s, respectively. In the Region 2 and 4, the annual precipitation showed a decreased trend before late 1980s, and significantly increased during 1990s. In the Region 5, the annual precipitation exhibited a variation with "saddle shape" during 1960–1980, then decreased during 1983–1999, and showed an increasing trend after 1999. As can be seen in Fig. 11, the increasing trend of annual precipitation did not exceed the 95% confidence level since 2000 in the most regions of the Tianshan Mountains.

5.2. Changes in large scale atmospheric circulation

Atmospheric circulation patterns are key factor for the long-term variation of temperature and precipitation (Sun et al., 2016; Wen et al., 2017). The result of mutation indicated that rapid warming started in 1990s in the Tianshan Mountains. To investigate the impacts of large scale circulation changes on climate change, we calculated the circulation map using NCEP/NCAR reanalysis data during 1960–1994 and 1995–2016, respectively, the former were subtracted from the latter to detect the changes in circulation between the two periods (Fig. 12). As shown on the geopotential height composite, enhanced anticyclonic circulation developed in most part of the Tianshan Mountains and the largest differences were located at 44°N and 98°E at 500 hPa. The differences of geopotential height and wind speed at 500 hPa between 1995–2016 and 1960–1994 indicate that the study area is located after an anomaly high pressure and also controlled by the bottom of an anomaly low pressure. This kind of atmospheric mode blocked the northward cold air, which in turn, provided favorable environment for the increasing temperature in the study area. The increased geopotential height over Central Asia was consistent with rapid warming in the northwest region of China which includes our study area (Deng et al., 2014). The water vapor in the Tianshan Mountains is largely transported to the area by the Westerly Circulation. The increased downward longwave radiation induced the net surface radiation to increase,

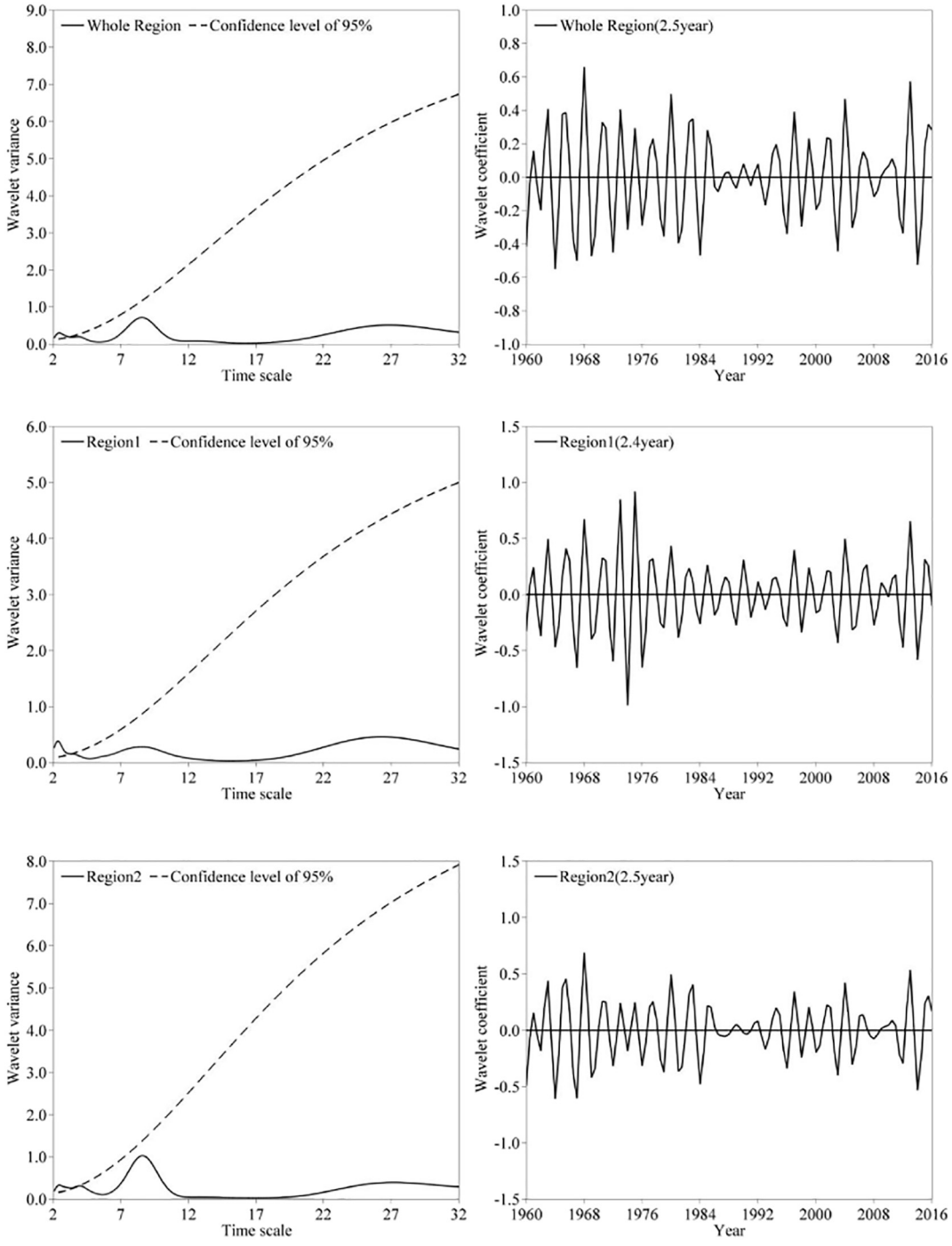

Fig. 13. Wavelet analyses of the annual air temperature in the Tianshan Mountains and sub-regions during the study period.

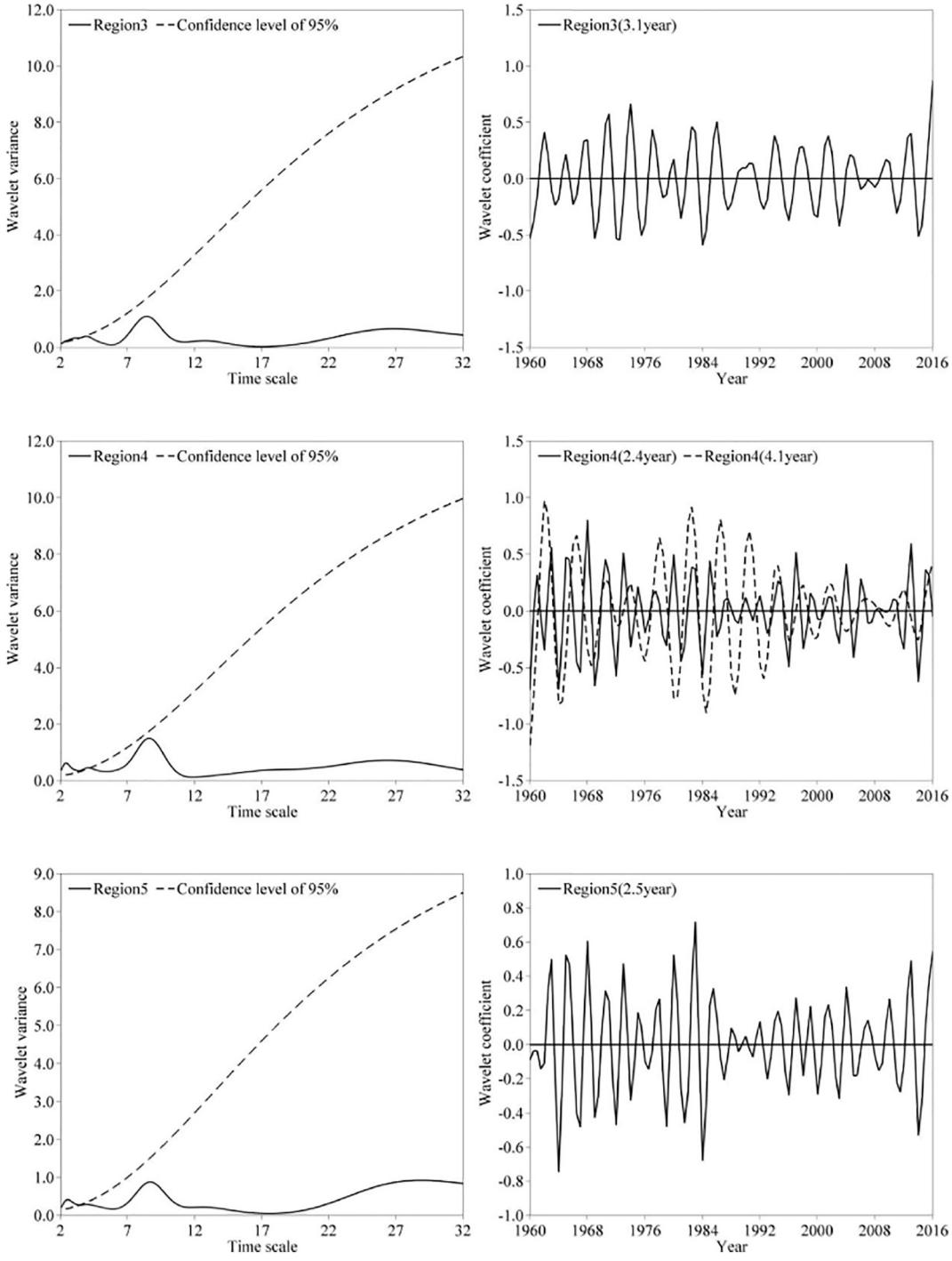

Fig. 13. (*continued*)

and supplied more energy to favor the evaporation process of vaporization (Ren et al., 2016). Previous study indicated that the sum of horizontal moisture advection and wind convergence terms has a significant positive contribution to the wetting trend in the northwest region of China (Peng and Zhou, 2017). As shown in Fig. 12, the southwestern wind at the bottom of the anomaly anticyclone drive the vapor flux from the Tarim river into the study area, which in turn, increases the precipitation. The precipitation increased obviously after 1990 (Fig. 11). The previous study indicated that the annual precipitation revealed strong and significant associations with the West Pacific Subtropical High and the North America Subtropical High in the northwest region of China (Li et al., 2016). Therefore, the strengthening anticyclone circulation, increasing geopotential height, and rapid warming have contributed to the changes in precipitation.

5.3. Periodic variations of climate change over the Tianshan Mountains

The Morlet wavelet can reveal the periodicity of high and low indexes of annual air temperature and precipitation, which was used to analyze the phase change and the periodic intensity on different time

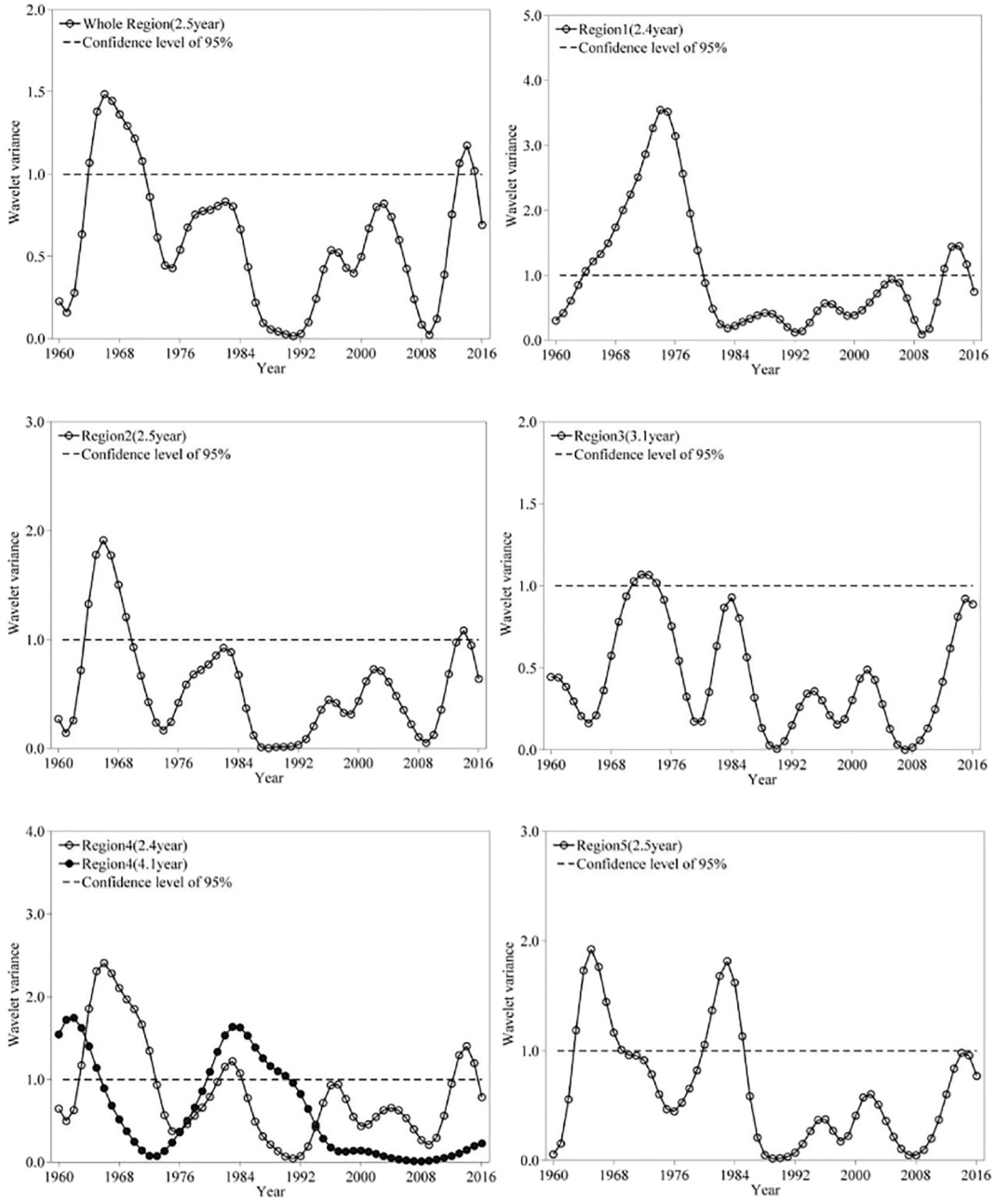

Fig. 14. Significant time sections of significant periodicities in the annual air temperature over the Tianshan Mountains and sub-regions during.

scales (Ling et al., 2013a, 2013b). However, the results of wavelet analyses in previous study were not specific as significance tests in period (He et al., 2013; Zhang et al., 2014). The significance of wavelet variances using a chi-square test was considered in this study, which was characterized by timeliness to limit certain sections. The periodic variations in annual air temperature were calculated using Eqs. (11)–(13). The wavelet variances, wavelet coefficients and significant time sections of annual air temperature were obtained using a Morlet wavelet function and are shown in Figs. 13 and 14. The wavelet variance of high and low indexes for annual air temperature in the whole Tianshan Mountains had a significant 2.5-year periodicity on the basis of a chi-square test at a confidence level of 95%. Besides, there also existed the main periods of 9.1-year and 25.3-year, which did not pass confidence level of 95%. According to the wavelet red-noise test at a confidence level of 95%, the most significant periodic fluctuation had a 2.5-year period and occurred during 1964–1971 and 2013–2015 in the Tianshan Mountains (Fig. 14). There was a significant 2.4-year periodicity in the Region 1 in 1964–1980 and 2012–2015 at a confidence level of 95%. The 95% significance level regions indicated intervals of higher variance from 1964 to 1970 with a 2.5-year periodicity in the Region 2. In the Region 3, the significant periodicity was 3.1-years, which had a high frequency of occurrence during 1960s. In the Region 4, there were two significant periods with 2.4-year and 4.1-year at a confidence level of 95%. The 2.4-year fluctuation of the wavelet variance was significant during 1963–1973, and the fluctuation of 4.1-year periodicity was significant during 1960–1965 and 1980–1992. The Region 5 presented a significant 2.5 year periodicity that occurred from 1963 to 1973 and from 1980 to 1985. The annual air temperature

showed 2.4–4.1 year periodicity in the Tianshan Mountains. The periodic variation of annual air temperature was stronger before 1990. The significant sections of periodicity occurred in different time series, which indicated that there were differing patterns of annual air temperature in the different regions of the Tianshan Mountains.

Figs. 15 and 16 show the phase change and the periodic intensity of annual precipitation on different time scales. In the whole Tianshan Mountains, the peak values of wavelet variance for precipitation were for 2.8 and 5.7 years at a confidence level of 95%, which meant that the significant periods were 2.8 and 5.7 years. The 2.8-year fluctuation of the wavelet variance was significant during 1964–1970, 1994–2000 and 2008–2014, and the 5.7-year fluctuation was significant during 1980–2016. The periodicity in Region 1 within 2.5-year and 7.4-year scale was detected, the significant periodicity of 2.5-year occurred in 1971–1978, 1994–2001 and 2005–2012 at a confidence level of 95%, the 7.4-year occurred during 1975–2016. In the Region 2, there existed significant 2.9-year periodicity during 1963–1969, 1985–1989, 1995–2000 and 2006–2014, the 5.5-year periodicity occurred during 1965–1973 and 1981–2016. The 95% significance level regions indicated intervals of higher variance with a 2.5-year periodicity and a 3.9-year periodicity in the Region 3. The significant time sections of 2.5-year periodicity occurred from 1962 to 1968, from 1981 to 1985

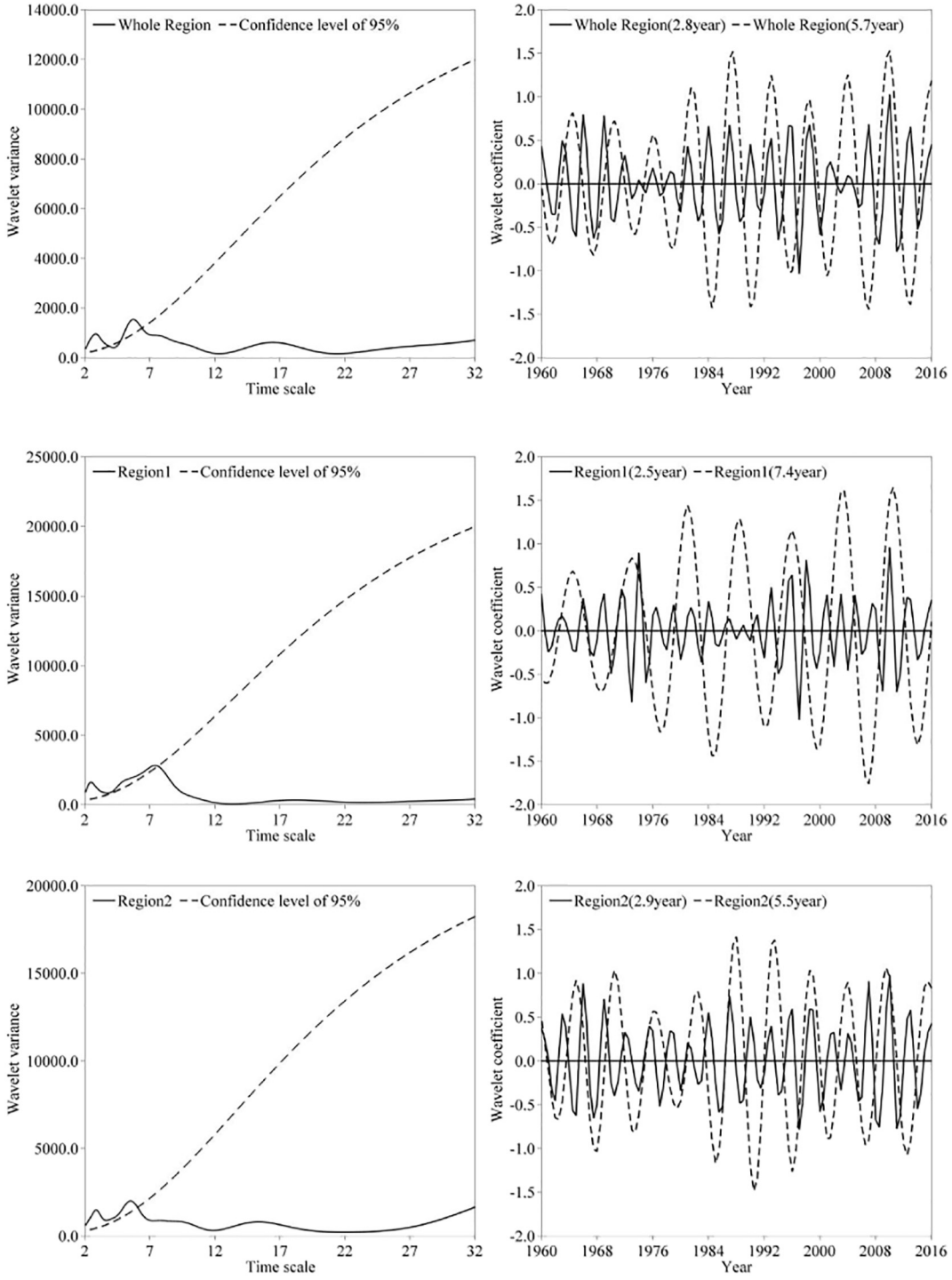

Fig. 15. Wavelet analyses of the annual precipitation in the Tianshan Mountains and sub-regions during the study period.

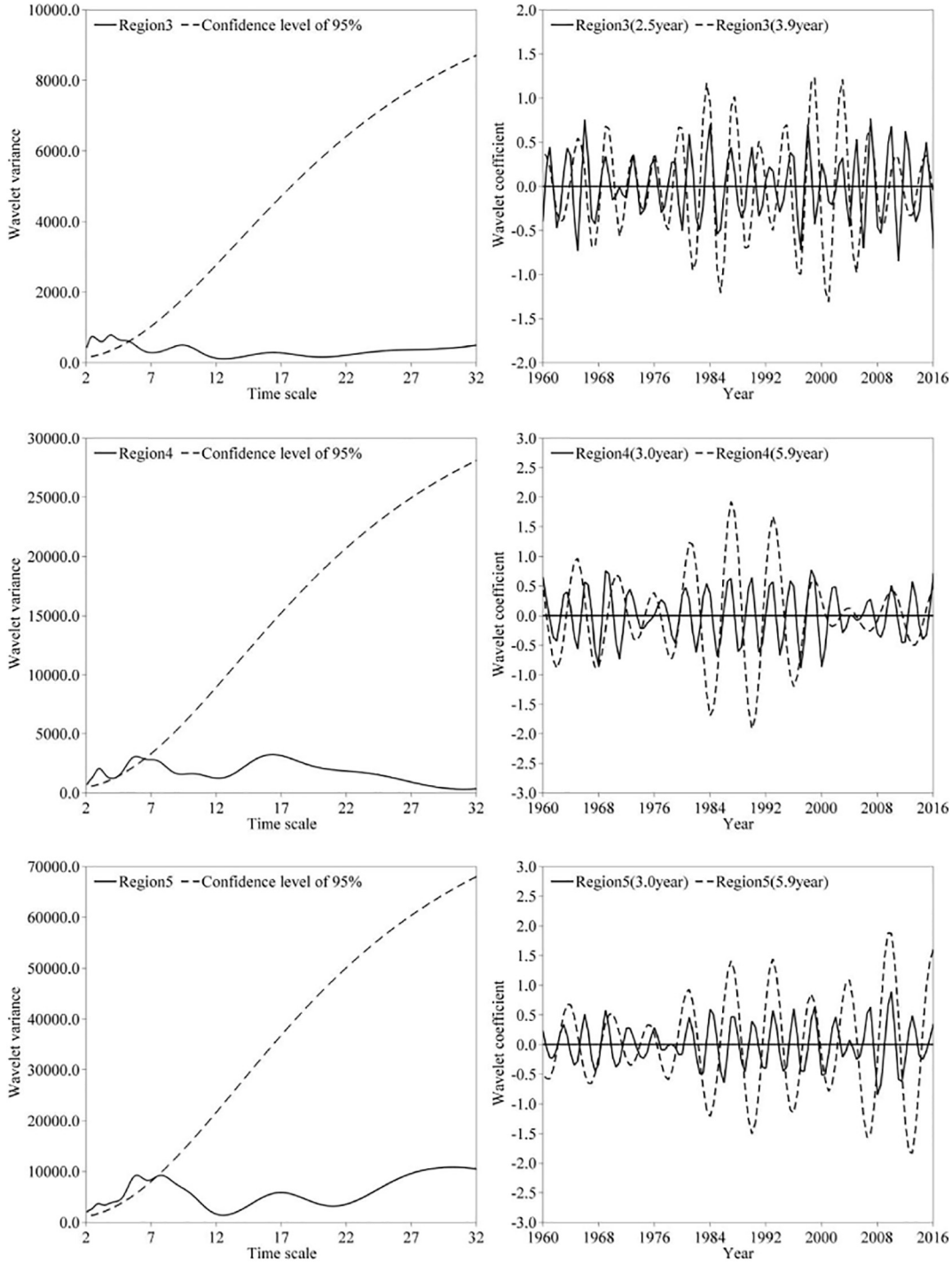

Fig. 15. (*continued*)

and from 1996 to 2014, and 3.9-year periodicity occurred from 1967 to 1970, from 1980 to 1990, and from 1995 to 2006. In the Region 4 and Region 5, the periodicity for annual precipitation showed significant at 3.0-year and 5.9-year, although the significant time sections showed differently. Overall, there were significant periods of annual precipitation with 2.5–7.4-years in the Tianshan Mountains. The periodic variation of annual precipitation was stronger after 1980. The fluctuation of annual precipitation showed more diverse significant periodicity than annual air temperature.

5.4. Relationship between trends of climate change and altitudes

Understanding of whether elevation dependent warming is of utmost interest for understanding the global climate change. Previous studies indicated that the warming at higher-elevation sites is more pronounced than that at lower elevations (Aizen, 1997; Beniston et al., 1997; Li et al., 2017). However, other studies also suggested that lack of any clear relationship between trend magnitude of air temperature and elevation (Vuille et al., 2003; Pepin and Norris, 2005; You et al., 2008,

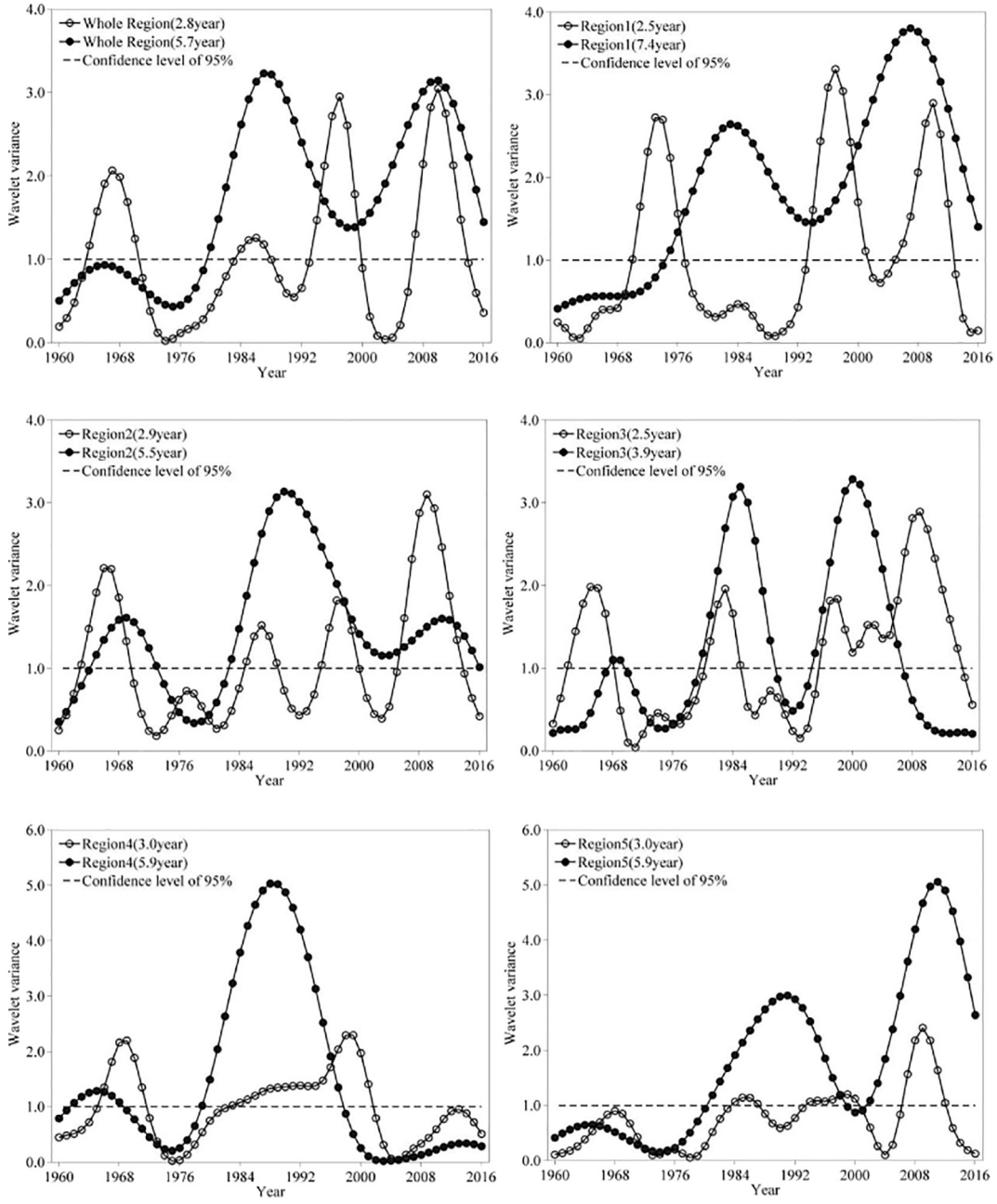

Fig. 16. Significant time sections of significant periodicities in the precipitation over the Tianshan Mountains and sub-regions during.

2010). As shown in Fig. 17, there are slight negative correlations between annual air temperature trend magnitude and elevation for spring, autumn, winter and annual in the Tianshan Mountains, but they are not significant. The only positive relationship occurs in summer. The relationship between trend magnitudes and elevation is not clear. This suggests that the altitude effect of annual air temperature were not evidently over the Tianshan Mountains. The enhancing warming in low altitude might be related to a large proportion of low-elevation valleys. On other hand, the meltwater of glaciers originating from the Tianshan Mountains and precipitation runoff could form some lakes in the region of lower elevation. Mediated by the fluxes of energy, moisture, and momentum, the lakes significantly alter the surface energy and then influence on regional climate (Anyah et al., 2010; Thiery et al., 2015). During summer, the lake-induced cooling happens in lower elevation, the lakes absorb incoming solar radiation and inhibit upward turbulent heat transport, the humid air has a lower probability of being heated by latent heat released from condensation at low elevations which induce lower trend in lower elevation. During cooler season (spring, autumn and winter), heat is released, the lakes warm near air which showed a greater trend magnitudes in lower elevation. The other reason is the meteorological stations in high-elevation are sparse and the highest elevation of station is 3504 m (TG).

Some researchers found an increasing amount of precipitation with altitude increasing in the mountain (Giorgi et al., 1997; Guo et al., 2016; Liu et al., 2011). Fig. 18 shows the relationships between annual precipitation trend magnitude and elevation in the Tianshan Mountains. There were slight negative correlations between precipitation trend magnitude and elevation for spring and winter, and they are not

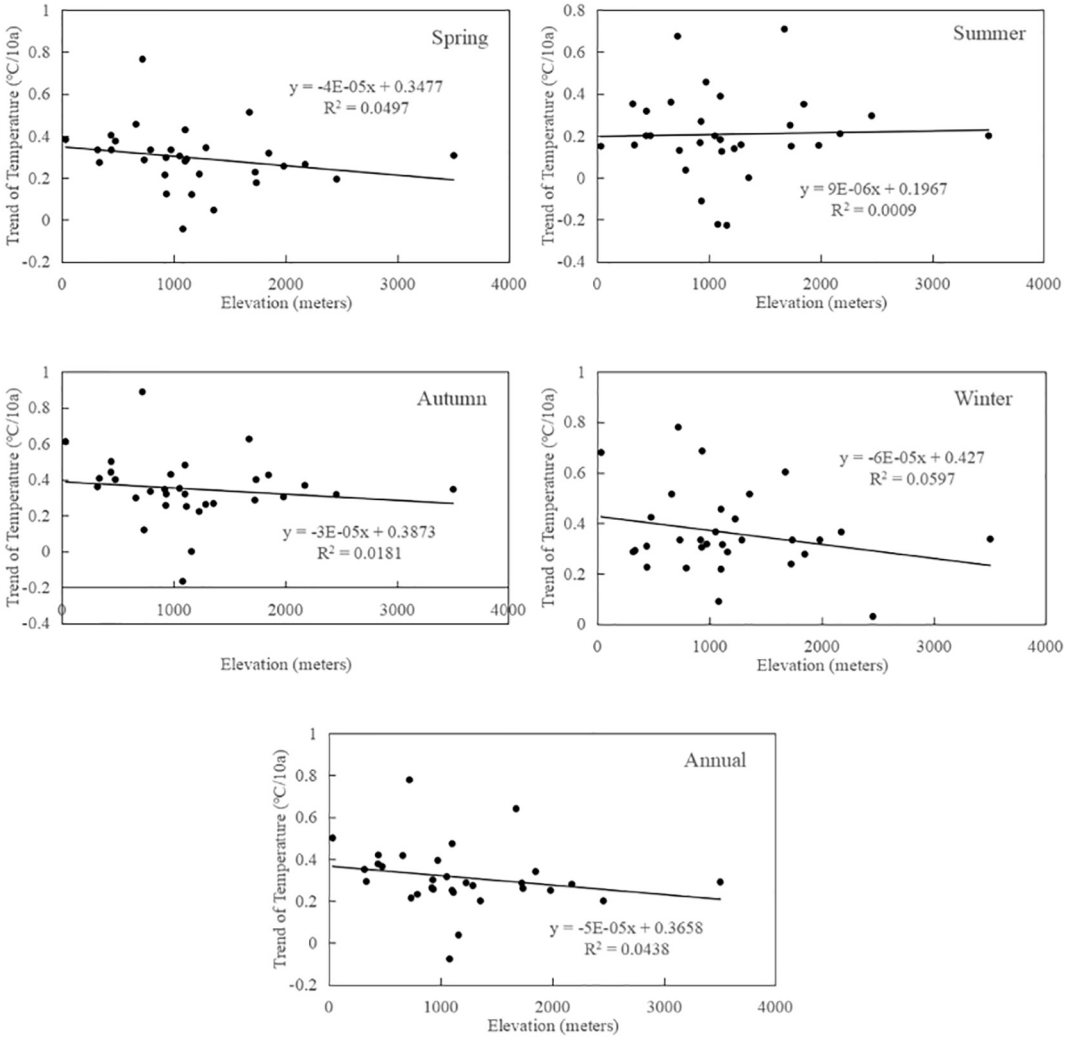

Fig. 17. Relationships between annual air temperature trend magnitude and elevation in the Tianshan Mountains.

significant. There exist positive relationships between the precipitation increased rates with the elevation for summer, autumn and annual. The strong elevation dependence in precipitation increased rates appeared in summer with a correlation efficient of 0.49 which is statistically significant at the 99% confidence level. The trend in summer precipitation from 1960 to 2010 displayed an increasing tendency at a rate of 2.6 mm/10a km^{-1} with the increased elevation. The annual precipitation wetting trend was amplified with elevation in summer and autumn in the Tianshan Mountains, which indicated the high mountainous areas experience more rapid changes in precipitation than that areas at lower elevations. The elevation dependency of annual and seasonal precipitation trend is far complex. However, the identified elevation dependence of the summer precipitation trends is in line with the increasing trends of air temperature with elevation. The Clausius-Clapeyron relationship indicated the changes in air temperature would lead to increased water vapor (Trenberth, 2011). The warmer air can hold more water vapor based on the Clausius-Clapeyron relationship, which makes it more likely to generate more precipitation. Annual precipitation trend magnitude decreased with elevation increasing in dry season, and increased with elevation increasing in wet season.

6. Conclusions

The temporal-spatial characteristics of air temperature and precipitation in the Tianshan Mountains were analysed based on 31 meteorological stations during 1960–2016. The conclusions can be summarized as follows:

(1) The Tianshan Mountains experienced an overall rapid warming and wetting during study period. The air temperature increase rate was 0.32 °C/10a. Annual mean air temperature has increased by around 1.82 °C from 1960 to 2016. Warming is the most significant in winter with an average rate of 0.32 °C/10a and the smallest in spring (0.27 °C/10a). Except KC station, the annual air temperature at all 30 stations showed a significant positive trend ($p < 0.05$). The spatial variation of temperature showed differently in annual and seasonal scale. The annual precipitation increased with a rate of 5.82 mm/10a during study period. Annual mean precipitation has increased by around 33.2 mm. In spatial distribution, the annual precipitation of 20 stations (64%) showed a non-significant upward trend.

(2) The temperatures of the Region 3 in the East Tianshan increased most rapidly at rates of 0.41 °C/10a. The rates increased gradually from west to east and were higher on the north slope than on the south slope. The increasing magnitudes of annual precipitation were highest in the Region 4 (Boertala Vally) and lowest in the Region 3 (East Tianshan). The precipitation change rate increased from the low-value area (Region 3) in the East Tianshan to the high-

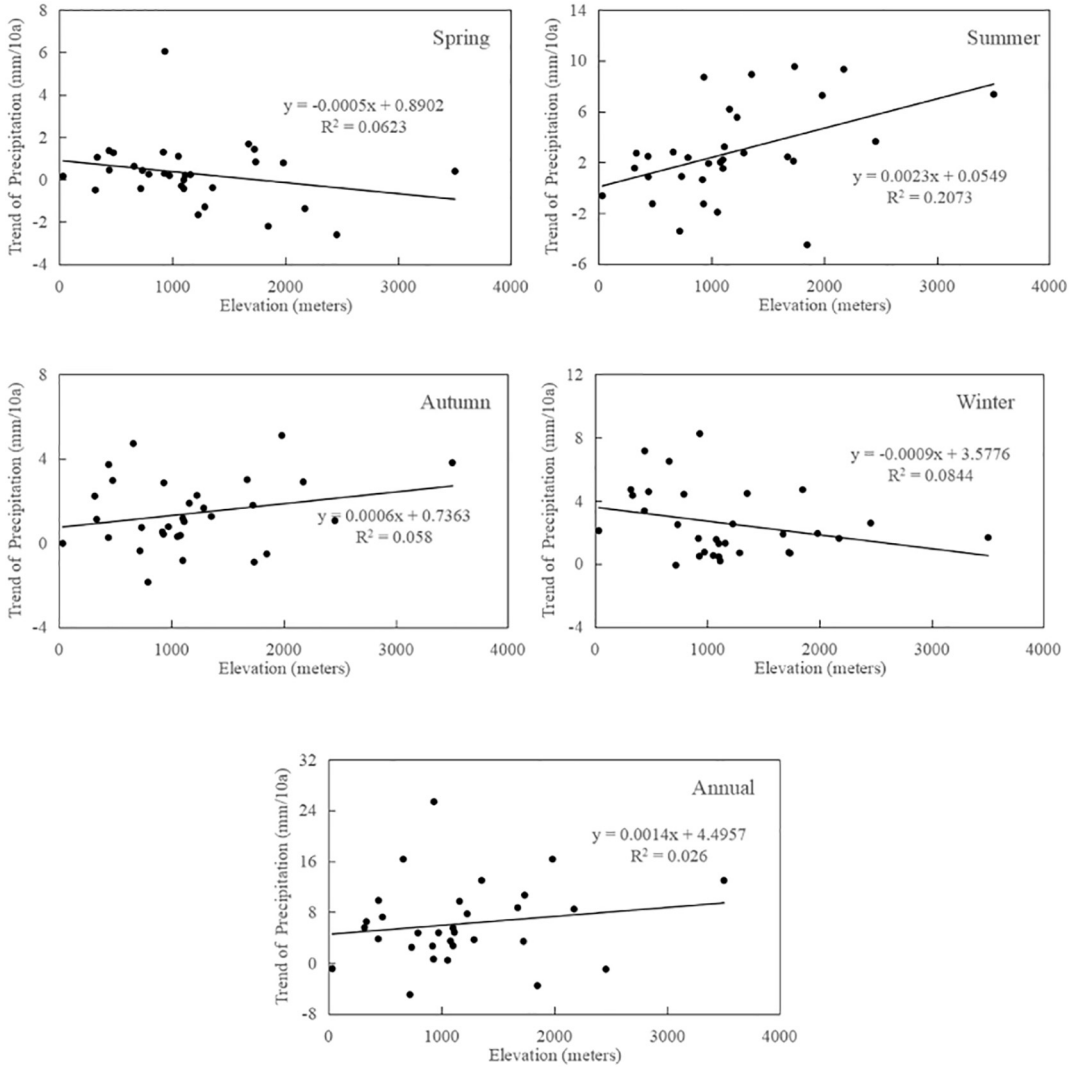

Fig. 18. Relationships between annual precipitation trend magnitude and elevation in the Tianshan Mountains.

value area (UQ) in the Middle Tianshan (Region 2), and the rate then decreased in the West Tianshan, although the value was higher than that in the eastern part. The greatest and weakest warming was below 500 m (0.42 °C/10a) and elevation of 1000–1500 m (0.23 °C/10a), respectively. The higher variability of temperature was observed in the elevation of 1500–2000 m and above 2000 m. The increasing magnitudes of annual precipitation were highest in the elevation of 1500 m–2000 m (9.22 mm/10a) and lowest in the elevation of below 500 m (3.45 mm/10a).

(3) The mutations of annual air temperature and precipitation in the Tianshan Mountains occurred in 1994 and 1982, respectively. The changes of the atmospheric circulation influenced on the mutations of climate in the study area during 1960–2016, anomaly high pressure and low pressure blocked the northward cold air which provided favorable environment for the increasing temperature in the study area. Moreover, the southwestern wind at the bottom of the anomaly anticyclone drive the vapor flux from the Tarim river into the study area, which in turn, increases the precipitation.

(4) The annual air temperature showed 2.4–4.1-year cycle in the Tianshan Mountains. There were significant periods of annual precipitation with 2.5–7.4-year. The different sub-regions in annual air temperature and precipitation showed different mutation. The periodic variation of annual air temperature and precipitation were evidently before 1990 and after 1980, respectively. The fluctuation of annual precipitation showed more diverse significant periodicity than annual air temperature.

(5) The elevation dependency of temperature increasing trend was not evidently in the Tianshan Mountains. The relationship between air temperature trend magnitude and elevation for spring, autumn, winter and annual showed slight negative correlations, and positive relationship occurs in summer. The lake-induced cooling happens during summer in lower elevation. The strong elevation dependence in precipitation increased rates appeared in summer. The annual precipitation wetting trend was amplified with elevation increasing in summer and autumn in the Tianshan Mountains, which indicated the high mountainous areas experience more rapid changes of wetting.

Acknowledgments

The authors would like to thank the editors and the anonymous reviewers for their crucial comments, which improved the quality of this paper. This study was supported by the National Natural Science Foundation of China (41421061, 41501073, 41690141, 41471060,

41771087), the project of State Key Laboratory of Cryospheric Science (SKLCS-ZZ-2017).

References

Aizen, V.B., 1997. Climatic and hydrologic changes in the Tien Shan, Central Asia. J. Clim. 10, 1393–1404.

Aizen, V.B., Aizen, E.M., Melack, J.M., 1995. Climate, snow cover, glaciers, and runoff in the Tien Shan, Central Asia. J. Am. Water Resour. As. 31, 1113–1129.

Alexander, L., Zhang, X., Peterson, T., Caesar, J., Gleason, B., Klein Tank, A., Haylock, M., Collins, D., Trewin, B., Rahimzadeh, F., 2006. Global observed changes in daily climate extremes of temperature and precipitation. J. Geophys. Res. Atmos. 111, D05109.

Anyah, R.O., Semazzi, F.H.M., Xie, L., 2010. Simulated physical mechanisms associated with climate variability over Lake Victoria basin in east Africa. Mon. Weather Rev. 134 (134), 3588–3609.

Beniston, M., Diaz, H.F., Bradley, R.S., 1997. Climatic change at high elevation sites: an overview. Clim. Chang. 36 (3–4), 233–251.

Berger, W.H., Labeyrie, L.D., 1985. Abrupt Climatic Change Evidence and Implications. St. Hugues de Biviers, France, pp. 8.

Blandford, T.R., Humes, K.S., Harshburger, B.J., Moore, B.C., Walden, V.P., Ye, H.C., 2008. Seasonal and synoptic variations in near-surface air temperature lapse rates in a mountainous basin. J. Appl. Meteorol. Climatol. 47 (1), 249–261.

Bothe, O., Fraedrich, K., Zhu, X.H., 2012. Precipitation climate of Central Asia and the largescale atmospheric circulation. Theor. Appl. Climatol. 108 (3–4), 345–354.

Brutsaert, W., Parlange, M.B., 1998. Hydrologic cycle explains the evaporation paradox. Nature 396 (6706), 30.

Chen, Y.N., Pang, Z.H., Hao, X.M., Xu, C.C., Chen, Y.P., 2008. Periodic changes of stream flow in the last 40 years in Tarim River Basin, Xinjiang, China. Hydrol. Process. 22, 4214–4221.

Chen, Y., Deng, H., Li, B., et al., 2014. Abrupt change of temperature and precipitation extremes in the arid region of Northwest China. Quat. Int. 336, 35–43.

Chen, Y., Li, Z., Fan, Y., Wang, H., Deng, H., 2015. Progress and prospects of climate change impacts on hydrology in the arid region of northwest China. Environ. Res. 139, 11–19.

Chen, Y.N., Li, H.W., Deng, H.J., Fang, G.H., Li, Z., 2016. Changes in central Asia's water tower: past, present and future. Sci. Rep. 6, 35458.

Crowley, T.J., 2000. Causes of climate change over the past 1000 years. Science 289 (5477), 270.

Deng, H., Chen, Y., Shi, X., Li, W., Wang, H., Zhang, S., 2014. Dynamics of temperature and precipitation extremes and their spatial variation in the arid region of northwest china. Atmos. Res. 138 (3), 346–355.

Deng, H.J., Chen, Y.N., Wang, H.J., Zhang, S.H., 2015. Climate change with elevation and its potential impact on water resources in the Tianshan Mountains, Central Asia. Glob. Planet. Chang. 135, 28–37.

Du, J., Ma, Y., 2004. Climatic trend of rainfall over Tibetan plateau from 1971 to 2000. Acta Geograph. Sin. 61 (7), 687–696 (in Chinese).

Du, J., Zhou, S., Tang, S., 2000. Analysis on the climatic characteristics of temperature variation in Tibet during the past 40 years. Quarterly Journal of Applied Meteorology 11 (2), 221–227.

Easterling, D.R., Horton, B., Jones, P.D., Peterson, T.C., Karl, T.R., Parker, D.E., 1997. Maximum and minimum temperature trends for the globe. Science 277 (5324), 364–367.

Gao, G., Chen, D., Xu, C.Y., Simelton, E., 2007. Trend of estimated actual evapotranspiration over china during 1960–2002. J. Geophys. Res. 112 (D11), 71–81.

Gao, T., Wang, H.J., Zhou, T., 2017. Changes of extreme precipitation and nonlinear influence of climate variables over monsoon region in china. Atmos. Res. 197, 379–389.

Gay-Garcia, C., Estrada, F., Sanchez, A., 2009. Global and hemispheric temperatures revisited. Clim. Chang. 94, 333–349.

Giorgi, F., Hurrell, J.W., Marinucci, M.R., Beniston, M., 1997. Elevation dependency of the surface climate change signal: a model study. J. Clim. 10 (2), 288–296.

Gong, D.Y., Ho, C.H., 2002. The Siberian High and climate change over middle to high latitude Asia. Theor. Appl. Climatol. 72 (1–2), 1–9.

Grinsted, A., Moore, J.C., Jevrejeva, S., 2004. Application of the cross wavelet transform and wavelet coherence to geophysical time series. Nonlinear Process. Geophys. 11, 561–566.

Guo, L., Li, L., 2015. Variation of the proportion of precipitation occurring as snow in the Tian Shan Mountains, China. Int. J. Climatol. 35 (7), 1379–1393.

Guo, X., Wang, L., Tian, L., 2016. Spatio-temporal variability of vertical gradients of major meteorological observations around the Tibetan Plateau. Int. J. Climatol. 36 (4), 1901–1916.

Hansen, J., Sato, M., Ruedy, R., Lo, K., Lea, D.W., Medina-Elizade, M., 2006. Global temperature change. Proc. Natl. Acad. Sci. U. S. A. 103 (39), 14288–14293.

Hao, X.M., Chen, Y.N., Li, W.H., 2007. Impact of anthropogenic activities on the hydrologic characters of the mainstream of the Tarim River in Xinjiang during the past 50 years. Environ. Geol. 52, 1365–1375.

He, B., Miao, C., Shi, W., 2013. Trend, abrupt change, and periodicity of streamflow in the mainstream of yellow river. Environ. Monit. Assess. 185 (7), 6187.

Holden, J., Rose, R., 2011. Temperature and surface lapse rate change: a study of the UK's longest upland instrumental record. Int. J. Climatol. 31 (6), 907–919.

Hu, Wei, Yao, Lei, 2008. The trend analysis on Air Temperature and Evaporation in Chuche County during recent 40 years. Res. Soil Water Conserv. 15 (3), 93–95.

Intergovernmental Panel on Climate Change Fifth Assessment Report (IPCC AR5), 2013. Summary for Policymakers: The Physical Science Basis, Contribution of Working Group I to the IPCC Fifth Assessment Report Climate Change. http://en.wikipedia.org/wiki/IPCC_Fifth_Assessment_Report (Approved 27Sep2013.pdf).

Jia, W., He, Y., Li, Z., 2008. The regional difference and catastrophe of climatic change in Qilian mountains region. Acta Geograph. Sin. 63 (3), 257–269 (in Chinese).

Kendall, M.G., 1975. Rank Correlation Methods. Griffin, London.

Kendall, M.G., Stuart, A., 1973. The Advanced Theory By Statistics. Griffin, London.

Kousari, M.R., Zarch, A.A.M., Ahani, H., Hakimelahi, H., 2013. A survey of temporal and spatial reference crop evapotranspiration trends in Iran from 1960 to 2005. Clim. Chang. 120, 277–298.

Li, Z., He, Y., Wang, C., Wang, X., Xin, H., Zhang, W., 2011. Spatial and temporal trends of temperature and precipitation during 1960–2008 at the Hengduan Mountains, China. Quat. Int. 236 (1–2), 127–142.

Li, B.F., Chen, Y.N., Chen, Z.S., Li, W.H., 2012a. Trends in runoff versus climate change in typical rivers in the arid region of northwest china. Quat. Int. 282, 87–95.

Li, B., Chen, Y., Shi, X., 2012b. Why does the temperature rise faster in the arid region of northwest China? J. Geophys. Res. 117 (D16), 16115.

Li, Z., Chen, Y., Li, W., Deng, H., Fang, G., 2015. Potential impacts of climate change on vegetation dynamics in Central Asia. J. Geophys. Res. 120, 12345–12356.

Li, B., Chen, Y., Chen, Z., Xiong, H., Lian, L., 2016. Why does precipitation in northwest china show a significant increasing trend from 1960 to 2010? Atmos. Res. 167, 275–284.

Li, X., Wang, L., Guo, X., Chen, D., 2017. Does summer precipitation trend over and around the Tibetan Plateau depend on elevation? Int. J. Climatol. 37 (Suppl. 1), 1278–1284.

Ling, H.B., Xu, H.L., Fu, J.Y., 2013a. High- and low-flow variations in annual runoff and their response to climate change in the headstreams of the Tarim River, Xinjiang, China. Hydrol. Process. 27, 975–988.

Ling, H.B., Xu, H.L., Fu, J.Y., 2013b. Temporal and spatial variation in regional climate and its impact on runoff in Xinjiang, China. Water Resour. Manag. 27, 381–399.

Lioubimtseva, E., Cole, R., Adams, J.M., Kapustin, G., 2005. Impacts of climate and land-cover changes in arid lands of Central Asia. J. Arid Environ. 62 (2), 285–308.

Liu, B., Feng, J., Ma, Z., 2009. Characteristics of climate changes in Xinjiang from 1960 to 2005. Clim. Environ. Res. 14 (4), 414–426 (in Chinese).

Liu, J.F., Chen, R.S., Qin, W.W., Yang, Y., 2011. Study on the vertical distribution of precipitation in mountainous regions using TRMM data. Adv. Water Sci. 22, 447–454 (in Chinese).

Liu, S.Y., Yao, X.J., Guo, W.Q., Xu, J.L., Shangguan, D.H., Wei, J.F., Bao, W.J., Wu, L.Z., 2015. The contemporary glaciers in china based on the second Chinese glacier inventory. Acta Geograph. Sin. 70, 3–16 (in Chinese).

Mahlstein, I., Knutti, R., 2010. Regional climate change patterns identified by cluster analysis. Clim. Dyn. 35 (4), 587–600.

Matyasovszky, I., 2011. Detecting abrupt climate changes on different time scales. Theor. Appl. Climatol. 105 (3–4), 445–454.

New, M., Todd, M., Hulme, M., Jones, P., 2001. Precipitation measurements and trends in the twentieth century. Int. J. Climatol. 21 (15), 1889–1922.

Ozturk, T., Turp, M.T., Türkeş, M., Kurnaz, M.L., 2017. Projected changes in temperature and precipitation climatology of Central Asia CORDEX Region 8 by using RegCM4.3.5. Atmos. Res. 183, 296–307.

Panagiotopoulos, F., Shahgedanova, M., Hannachi, A., Stephenson, D.B., 2005. Observed trends and teleconnections of the Siberian high: a recently declining center of action. J. Clim. 18 (9), 1411–1422.

Peng, D., Zhou, T., 2017. Why was the arid and semiarid northwest China getting wetter in the recent decades? J. Geophys. Res. 122.

Pepin, N.C., Norris, J., 2005. An examination of the differences between surface and free air temperature trend at high elevation sites: relationships with cloud cover, snow cover and wind. J. Geophys. Res. 110, D24112.

Piao, S.L., Ciais, P., Huang, Y., Shen, S., Peng, S., Li, J., Zhou, L., Liu, H., Ma, Y., Ding, Y., Friedlingstein, P., Liu, C., Tan, K., Yu, Y., Zhang, T., Fang, J., 2010. The impacts of climate change on water resources and agriculture in China. Nature 467, 43–51.

Qi, J., Kulmatov, R., 2008. An overview of environmental issues in Central Asia. In: Qi, J., Evered, K. (Eds.), Environmental problems of Central Asia and their economic, social and security impacts. NATO science for peace and security series C: Environmental security. Springer, Netherlands, pp. 3–14.

Ren, G.Y., Yuan, Y.J., Liu, Y.J., Ren, Y.Y., Wang, T., Ren, X.Y., 2016. Changes in precipitation over northwest China. Arid Zone Res. 33 (1), 1–19 (in Chinese).

Sorg, A., Bolch, T., Stoffel, M., Solomina, O., Beniston, M., 2012. Climate change impacts on glaciers and runoff in Tien Shan (central Asia). Nat. Clim. Chang. 2, 725–731.

Souleymane, F., Anthony, W., John, N., Evan, J., Dev, N., Christy, J.R., 2011. Analysis of the impacts of station exposure on the U.S. historical climatology network temperatures and temperature trends. J. Geophys. Res. 116 (D14), 811–840.

Sun, L., Yin, Y., 2010. Change of precipitation distribution and trends in China from 1960–2009. In: The 27th Annual Meeting of China Meteorological Society Proceedings of Atmospheric Physics and Atmospheric Conditions at the Venue, Beijing.

Sun, W., Mu, X., Song, X., Wu, D., Cheng, A., Qiu, B., 2016. Changes in extreme temperature and precipitation events in the Loess Plateau (China) during 1960–2013 under global warming. Atmos. Res. 168 (22), 33–48.

Thiery, W., Panitz, H., Van Lipzig, N., 2015. The impact of the African great lakes on the regional climate in a dynamically downscaled CORDEX simulation (COSMO-CLM). J. Clim. 28 (10), 4061–4085.

Torrence, C., Compo, G.P., 1998. A practical guide to wavelet analysis. B. Am. Meteorol. Soc. 79, 61–78.

Trenberth, K.E., 2011. Changes in precipitation with climate change. Clim. Res. 47 (47), 123–138.

Vuille, M., Bradley, R.S., Werner, M., Keimig, F., 2003. 20th century climate change in the

tropical Andes: observations and model results. Clim. Chang. 59, 75–99.
Wang, S.J., Zhang, M.J., Li, Z.Q., Wang, F.T., Li, H.L., Li, Y.J., Huang, X.Y., 2011. Glacier area variation and climate change in the Chinese Tianshan Mountains since 1960. J. Geogr. Sci. 21, 263–273.
Wang, X., Yang, M., Liang, X., Pang, G., Wan, G., Chen, X., 2013. The dramatic climate warming in the Qaidam Basin, northeastern Tibetan Plateau, during 1961–2010. Int. J. Climatol. 34 (5), 1524–1537.
Wen, X., Wu, X., Gao, M., 2017. Spatiotemporal variability of temperature and precipitation in Gansu Province (northwest china) during 1951–2015. Atmos. Res. 197, 132–149.
Xi, C., Luo, G., Xia, J., Zhou, K., Lou, S., Ye, M., 2005. Ecological response to the climate change on the northern slope of the Tianshan mountains in Xinjiang. Sci. China Earth Sci. 48 (6), 765–777.
Xu, M., 2017. Study on water storage change and its consideration in water balance in the mountain regions over arid northwest China. Adv. Meteorol. 7, 1–10.
Xu, M., Han, H., Kang, S.C., 2017a. Modeling glacier mass balance and runoff in the Koxkar River Basin on the south slope of the Tianshan Mountains, China, from 1959 to 2009. Water 9 (2), 100.
Xu, M., Wu, H., Kang, S.C., 2017b. Impacts of climate change on the discharge and glacier mass balance of the different glacierized watersheds in the Tianshan Mountains, Central Asia. Hydrol. Process. http://dx.doi.org/10.1002/hyp.11409.
Yang, F., Lau, K., 2004. Trend and variability of china precipitation in spring and summer: linkage to sea-surface temperatures. Int. J. Climatol. 24 (24), 1625–1644.
Yang, X., Zhang, Y., Zhang, W., 2006. Climate change in Mt. Qomolangma region in China during the last 34 years. Acta Geograph. Sin. 61 (7), 687–696 (in Chinese).
Yang, K., Ye, B., Zhou, D., Wu, B., Foken, T., Qin, J., 2011. Response of hydrological cycle to recent climate changes in the Tibetan Plateau. Clim. Chang. 109 (3–4), 517–534.
Yang, H., Yang, D., Hu, Q., Lv, H., 2015. Spatial variability of the trends in climatic variables across china during 1961–2010. Theor. Appl. Climatol. 120 (3–4), 773–783.
Yao, J., Yang, Q., Mao, W., Zhao, Y., Xu, X., 2016. Precipitation trend-elevation relationship in arid regions of the China. Glob. Planet. Chang. 143, 1–9.
Ye, B.S., Yang, D.Q., Jiao, K.Q., Han, T.D., Jin, Z.F., Yang, H.A., Li, Z.Q., 2005. The Urumqi River source glacier no. 1, Tianshan, China: changes over the past 45 years. Geophys. Res. Lett. 32, 154–164.
You, Q., Kang, S.C., Pepin, N., Yan, Y.P., 2008. Relationship between trends in temperature extremes and elevation in the eastern and central Tibetan Plateau, 1961–2005. Geophys. Res. Lett. 35, L04704.
You, Q.L., Kang, S.C., Pepin, N., Flügel, W.A., Yan, Y.P., Behrawan, H., 2010. Relationship between temperature trend magnitude, elevation and mean temperature in the Tibetan Plateau from homogenized surface stations and reanalysis data. Glob. Planet. Chang. 71 (1–2), 124–133.
Zhang, Q., Singh, V.P., Li, K., Li, J., 2014. Trend, periodicity and abrupt change in streamflow of the east river, the pearl river basin. Hydrol. Process. 28 (2), 305–314.
Zhang, Y., Gao, Z., Pan, Z., Li, D., Huang, X., 2016. Spatiotemporal variability of extreme temperature frequency and amplitude in China. Atmos. Res. 185, 131–134.